Mathematical Modelling and Numerical Simulation with Applications, 2025, 5(2), 280–306

https://dergipark.org.tr/en/pub/mmnsa

ISSN Online: 2791-8564 / Open Access

https://doi.org/10.53391/mmnsa.1567457

RESEARCH PAPER

Temporal dynamics of immunity: modeling susceptibility delay in antibody-shielded populations

B. Krithika [1,‡] and **P. Tamilalagan** [1,*,‡]

[1]Department of Mathematics, Amrita School of Physical Sciences, Coimbatore, Amrita Vishwa Vidyapeetham, India

* Corresponding Author

‡ b_krithika@cb.students.amrita.edu (B. Krithika); p_tamilalagan@cb.amrita.edu (P. Tamilalagan)

Abstract

This study presents a mathematical model that incorporates multiple time delays and a distinct compartment for antibody-protected immune individuals to analyze the transmission dynamics of infectious diseases. We ensure through analytical results that our model produced positive and bounded solutions, which is essential for realistic predictions. Parameter estimation is performed using real-time data to accurately determine the time delays associated with the system. In the absence of time delays, the analysis demonstrates that the disease transmission rate (β) plays a critical role in determining the system's behavior. When β exceeds a threshold value (β_c), a forward bifurcation occurs. The study further investigates the impact of time delays on the stability of disease-free and endemic equilibria and identifies conditions under which the system undergoes a Hopf bifurcation, resulting in periodic oscillations. Numerical simulations are conducted to validate the theoretical findings, providing insights into the influence of immunity delays on disease persistence and intervention strategies.

Keywords: Mathematical model; epidemiology; dynamical systems; time-delay; Hopf bifurcation; stability

AMS 2020 Classification: 00A71; 92B05; 34H15; 34C23

1 Introduction

The global public health landscape continues to face formidable challenges posed by infectious diseases, necessitating the development of effective control strategies. Mathematical models are essential tools to understand the dynamics of disease transmission and to evaluate interventions. During the spread of epidemics, mathematical models have played a crucial role in making important public health decisions, like implementing curfews, especially when information about the disease or virus is limited. The models, such as Susceptible-Exposed-Infected-Recovered

➤ **Received:** 15.10.2024 ➤ **Revised:** 14.03.2025 ➤ **Accepted:** 12.06.2025 ➤ **Published:** 30.06.2025

(SEIR) or Susceptible-Infected-Recovered (SIR) types, take into account the factors like how long people are exposed to the disease and the impact of vaccination [1–16]. Researchers use these models to study the spread of deadly infectious diseases. For example, the authors in [4] proposed an epidemiological model and examined the role of asymptomatic testing and infection in the spread of the new coronavirus, highlighting the importance of asymptomatic carriers in disease transmission. In [17], the authors have proposed an epidemic model that incorporates a novel vaccination strategy by introducing a delay in the time it takes for vaccination to begin working effectively. This study mainly focused on exploring the influence of vaccination on disease control and the implementation of effective measures to mitigate disease spread, with particular emphasis on the basic reproduction ratio. The authors of [18] presented a new mathematical model to investigate the transmission dynamics of tuberculosis by taking vaccination into account and the time delay imposed by the latent phase of tuberculosis. In a similar manner, the authors in [19] developed a mathematical model by incorporating the time required for the vaccine to provide complete protection against Severe Acute Respiratory Syndrome Coronavirus-2 (SARS-CoV-2) through a set of delay differential equations.

The aforementioned research widely acknowledges the traditional emphasis in mathematical models on compartments representing susceptible, infected, and recovered individuals, assuming that the individuals possess complete immunity after recovery. For mathematical convenience, this assumption, known as "homogeneous immunity," has been utilized so far. The shortcomings of this presumption, however, have been highlighted by recent studies, underscoring the need for more realistic and multifaceted representations of immunity dynamics [20–23]. This becomes particularly important considering research suggesting that immunity may not last forever, regardless of how it was obtained - through vaccination or involuntary infection. Waning immunity poses significant implications for disease control and prevention strategies, necessitating a dynamic approach to modeling immunity [20–23]. For instance, empirical studies have documented the decrease in antibody levels over time, raising questions about the durability of immunity and the potential for reinfection [24–31]. Traditional models have focused on susceptible, infected, and recovered individuals, assuming that recovery provides complete and lasting immunity [26–36]. However, with new antibody-based interventions like monoclonal antibodies and vaccinations, it's crucial to account for varying levels and durations of protection provided by antibodies [37, 38]. In the realm of antibody-mediated immunity, a time delay emerges in the period required for immune individuals to become susceptible once again, often linked to the waning of antibody levels or the emergence of new pathogen strains. For instance, the authors in [20] provided a survey of "how long antibody responses last after COVID-19 infection?" and the gradual decrease of the antibodies over time. Incorporating these insights, our study introduces a unique contribution by explicitly accounting for the non-permanence of the immune class (A), reflecting a more realistic and dynamic understanding of immunity. This assumption is supported by a growing body of medical research indicating that antibody-mediated immunity may wane, necessitating the consideration of time delays in the susceptibility period for immune individuals. Such an approach allows for a more accurate modeling of disease transmission dynamics, especially in the context of ongoing epidemic diseases such as COVID-19, influenza [37, 38].

Among the various factors garnering increased attention, the presence of an antibody-protected immune subpopulation in the context of infectious diseases stands out as crucial. This subpopulation comprises individuals who have acquired passive immunity through the presence of antibodies, either via vaccination or natural infection. These individuals enjoy temporary protection against reinfection due to the presence of specific antibodies targeting the pathogen. By incorporating this antibody-protected compartment within mathematical models, one can capture the intricate dynamics of disease transmission and the effects of antibody-based interventions.

Also, the inclusion of time delays in disease modeling is essential for accurate understanding of diseases behaviour [39–44]. However, in the existing literature, there are no other articles that take into account the delay in the "period of susceptibility" for immune individuals, which refers to the time it takes for individuals with immunity to become susceptible to the disease again.
Building on the preceding discussions, our study introduces a distinctive contribution to the existing body of research by incorporating two pivotal factors: the presence of antibody-protected immune individuals and the consideration of a time delay, necessary for these immune individuals to revert to susceptibility. This, in fact, enables us to understand how the overall dynamics of the epidemic are influenced by antibody protection and the associated temporal time delay. Additionally, we have also included two more time lags: the time required for infectiousness to be detected and the duration it takes for an individual to receive the entire recommended dosage of vaccination. Furthermore, we have calibrated system parameters, including time delays, utilizing real-time COVID-19 data, thereby enhancing the realism of our results. Consequently, our research represents a noteworthy advancement in the mathematical modeling of infectious diseases, particularly within the context of COVID-19, offering a novel perspective on the dynamics of antibody-protected individuals and the temporal dynamics of their susceptibility.
The main objectives of this study are as follows:

- Investigating the robustness of immunity in the context of epidemic prevalence.
- Understanding the essential factors influencing disease behavior in the absence of time delays.
- Assessing how variations in delay parameters impact the spread of the disease.
- Exploring the influence of the delay in the period of susceptibility on the prevalence of the disease.

The subsequent sections of the article are structured as follows: In Section 2, we present a detailed description of the model, along with the associated biological assumptions to effectively validate its structure. The positivity and boundedness of the solutions are outlined in Section 3. In Section 3 (model equilibria and the basic reproduction number), we compute the model equilibria and determine the basic reproduction number. Section 3 (data fitting and calibration of model parameters) deals with data fitting and calibration of model parameters using real-time COVID-19 data. In Section 3 (time delay-free system dynamics: exploring parameter influences), we discuss "How the system behaves without delays?", and in Section 3 (System dynamics with time delays), we explore the system's dynamics in the presence of delays. In Section 4, we provide numerically simulated results that verify our theoretical analysis and demonstrate the application of the model to the COVID-19 pandemic under various scenarios. Finally, a concise discussion in Section 5 serves to conclude the manuscript.

2 Model formulation

The time-delayed model explored in this work is described as follows:

$$\begin{aligned}
\frac{dS(t)}{dt} &= (1-q)p - \frac{\beta S(t-\tau_1)I(t-\tau_1)}{N} - \mu S(t-\tau_2) + r_1 A(t-\tau_3) - \rho S(t),\\
\frac{dI(t)}{dt} &= \frac{\beta S(t-\tau_1)I(t-\tau_1)}{N} - (c+\rho_0)I(t),\\
\frac{dV(t)}{dt} &= qp + \mu S(t-\tau_2) - (k+\rho)V(t),\\
\frac{dR(t)}{dt} &= cI(t) - (r_2+\rho)R(t),\\
\frac{dA(t)}{dt} &= kV(t) - r_1 A(t-\tau_3) + r_2 R(t) - \rho A(t).
\end{aligned} \tag{1}$$

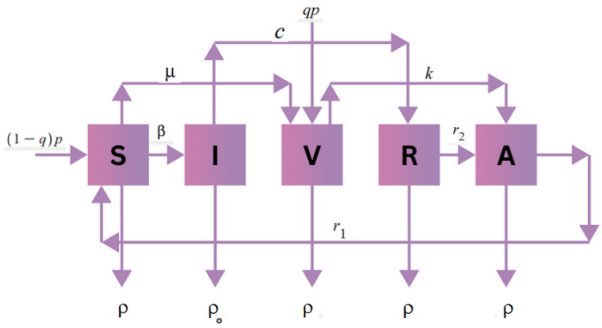

Figure 1. A schematic flow chart of the proposed model (1) is created in which the human host population is divided into 5 states namely Susceptible (S), Infected (I), Vaccinated (V), Recovered (R) and Immune (A). The transition of individuals between the population states and the direction of transmission are indicated by arrows

Here, the total human population (N) is divided into five compartments: Susceptible (S), Infected (I), Vaccinated (V), Recovered (R) and antibody-protected immune individuals as depicted in Figure 1. The description of the state variables are: $S(t)$ represents the proportion of individuals, who are susceptible or in a healthy state at time t, encompassing both healthy and non-vaccinated individuals; $I(t)$ represents the proportion of symptomatic infected individuals at time t; $V(t)$ represents the proportion of individuals, who have completed all the required doses of vaccination for the specific epidemic at time t, as numerous epidemics require multiple doses of vaccination to induce the full production of antibodies against infection [45–47]; $R(t)$ represents the proportion of individuals, who have recovered from the disease at time t; $A(t)$ represents the proportion of individuals, who acquires antibodies due to either by vaccination or recovery from a past infection. Our hypotheses regarding the transition of individuals from one state to another are outlined below. It is crucial to emphasize that, within the Eq. (1), we introduce a modified epidemic model that differs from the one outlined in [48] in the following manner:

- In the realm of epidemiology, the latent period refers to the duration during which the virus or pathogen replicates within the host and reaches a sufficient level for the individual to become capable of transmitting the disease to others. While a separate latent compartment may be suitable in some cases, a time delay parameter often adequately captures the essential characteristics of the latent period. This approach aligns with empirical observations and the biological understanding of infectious disease dynamics [2, 49]. Based on this, we introduce the parameter τ_1 as the time delay associated with the latent period, representing the duration between an individual's exposure to the infectious agent and the onset of infectiousness.
- In the work conducted by Cai et al. [48], it was asserted that individuals who had recovered from the disease were assumed to be susceptible to it once again. This proposition was further extended by Zhang et al. [29], who introduced a time delay associated with temporary immunity. The hypothesis posited that individuals with a history of recovery could regain susceptibility to the disease after a certain period due to partial or temporary immunity. Both models presented in [48] and [29] are formulated under the assumption that vaccinated individuals may be infected through direct exposure to infected individuals at a reduced rate compared to unvaccinated individuals. Additionally, research findings suggest that vaccines for numerous epidemics may necessitate repeated doses or booster shots to ensure extended protection [45–48, 50]. However, it is noteworthy that vaccines typically do not confer lifelong immunity. The levels of protection may naturally diminish over time or be compromised due to factors such as medical conditions, medications, or aging, during which the immune system may function

less effectively [51]. To address these considerations, we make the assumption that individuals who have not completed their vaccination regimen, including those who have received only a single dose, are considered susceptible to the disease. Furthermore, we introduce time delays τ_2 and τ_3 to account for the delay in completing vaccination and the period of susceptibility for antibody-protected immune individuals.

- Consequently, the susceptibility of recovered individuals in [29] has been generalized by incorporating the term $r_1 A(t-\tau_3)$ to signify the susceptibility of antibody-protected immune individuals who have gained immunity through both recovery and complete vaccination.
- We have also incorporated a mortality rate specific to the disease for infected individuals, diverging from the approach in [29, 48] where the mortality rate remains constant across all individual compartments.

The study is based on the following key assumptions:

- Instead of introducing a separate latent compartment, a time delay parameter (τ_1) is incorporated to represent the duration between exposure and the onset of infectiousness. This approach aligns with empirical observations of infectious disease dynamics.
- Individuals who recover from the disease are assumed to regain susceptibility after a certain period due to partial or temporary immunity. This is modeled using a time delay parameter (τ_3).
- Individuals who have not completed their full vaccination regimen, including those who have received only one dose, are considered susceptible to infection.
- Vaccinated individuals may still contract the disease, but at a reduced rate compared to unvaccinated individuals.
- Immunity from vaccination or natural infection is not lifelong and can diminish over time.
- Time delays (τ_2 and τ_3) are introduced to account for delays in completing vaccination and the period of susceptibility for antibody-protected individuals.
- A distinct mortality rate for infected individuals is considered, differing from models that assume a constant mortality rate across all compartments.
- The susceptibility of recovered individuals is generalized by incorporating a term that accounts for the transition of antibody-protected immune individuals back to the susceptible state.

The system parameters are described as follows:
p: Recruitment rate of susceptibles, q: Proportion of newborn individuals taking vaccination, μ: Complete vaccination rate of susceptibles, c: Recovery (cure) rate of infected individuals, k: Antibody development rate of fully vaccinated individuals, r_1: Rate of susceptibility of immune individuals, r_2: Antibody development rate of recovered individuals, ρ: Natural death rate of susceptibles, vaccinated, recovered and immune compartments, ρ_0: Disease mortality rate of infected individuals.

3 Dynamical characteristics of the model

Positivity and boundedness of solutions

Let τ=max$\{\tau_1, \tau_2, \tau_3\}$ and consider $\mathbb{R}^5_+ = \{(x_1, x_2, x_3, x_4, x_5)/x_i \geq 0, i = 1, 2, 3, 4, 5\}$. The initial conditions for the system (1) are given by

$$S(\theta) = \vartheta_1(\theta), \quad I(\theta) = \vartheta_2(\theta), \quad V(\theta) = \vartheta_3(\theta), \quad R(\theta) = \vartheta_4(\theta), \quad A(\theta) = \vartheta_5(\theta), \tag{2}$$

with $\vartheta_i(\theta) \geq 0$, $\vartheta_i(0) > 0$, $i = 1, 2, 3, 4, 5$; $\theta \in [-\tau, 0]$ and $(\vartheta_1, \vartheta_2, \vartheta_3, \vartheta_4, \vartheta_5) \in \mathcal{C}([-\tau, 0], \mathbb{R}^5_+)$. Where, $\mathcal{C}([-\tau, 0], \mathbb{R}^5_+)$ denotes the Banach space of continuous functions from the domain $[-\tau, 0]$

to $\mathbb{R}^5_+$ under Supremum norm. Then, it is obvious that the model equations in (1) with given initial history functions (2) has a unique solution.

Theorem 1 *If, $(S(t), I(t), V(t), R(t), A(t))$ is the solution of the model (1) with initial conditions (2) then, the compact set $\Phi = \left\{(S(t), I(t), V(t), R(t), A(t)) \in \mathbb{R}^5_+, N \leq \frac{p}{\rho}\right\}$ is positively invariant and attracts all solutions in $\mathbb{R}^5_+$.*

Proof First, we establish the non-negativity of solutions for system (1). If $\tau_1 < \tau_2 < \tau_3$, for $t \in [0, \tau_1]$, all delayed terms $S(t-\tau_1)$, $I(t-\tau_1)$, $S(t-\tau_2)$, and $A(t-\tau_3)$ refer to the initial conditions, which are non-negative. Hence, the derivatives of $S(t)$, $I(t)$, $V(t)$, $R(t)$, and $A(t)$ are non-negative whenever the respective function is zero, ensuring non-negativity in this interval. Extending this argument to $t \in [\tau_1, \tau_2]$, $t \in [\tau_2, \tau_3]$, and $t \geq \tau_3$ follows from the continuous dependence of solutions on initial conditions and the non-negative nature of the right-hand side functions in Eq. (1).
The total population $N(t) = S(t) + I(t) + V(t) + R(t) + A(t)$ satisfies:

$$\frac{dN(t)}{dt} \leq p - \widehat{\rho} N(t), \tag{3}$$

where, $\widehat{\rho} = \min\{\rho, \rho_0\}$. The Eq. (3) implies that $N(t)$ is bounded above by $\frac{p}{\widehat{\rho}}$ as $t \to \infty$, ensuring the set Φ is positively invariant and attracts all solutions in $\mathbb{R}^5_+$.

Model equilibria and the basic reproduction number

To explore the scenario where no infection persists, we enforce $I = 0$, leading to the identification of the disease-free equilibrium expressed as $\mathcal{E}_0 = \left(\frac{p\phi_3}{\phi_1}, 0, \frac{p\eta_5(\mu(1-q)+q\eta_1)}{\phi_1}, 0, \frac{pk(\mu(1-q)+q\eta_1)}{\phi_1}\right)$, where $\phi_1 = \eta_1\eta_3\eta_5 - k\mu r_1$, $\phi_2 = \eta_2\eta_4\eta_5 - cr_1r_2$, $\phi_3 = kqr_1 + (1-q)\eta_3\eta_5$, $\eta_1 = \mu + \rho$, $\eta_2 = c + \rho_0$, $\eta_3 = k + \rho$, $\eta_4 = r_2 + \rho$, and $\eta_5 = r_1 + \rho$.
Before exploring the calculation of the endemic equilibrium for our model (1), we first define a key threshold parameter, essential for assessing the model's qualitative dynamics.
The basic reproduction number, $\mathcal{R}_0$, for model (1) is derived using the next-generation matrix approach as outlined in [52] and [53]. The next generation matrix, K is defined as FV^{-1}. Here, F represents the rate of appearance of new infections in each compartment, and V accounts for the transitions out of infectious compartments due to recovery or death. The next generation matrix acts as a linear transformation that determines how infections propagate across generations. The spectral radius of K, denoted by $\widehat{\rho}(K)$, is the largest eigenvalue in magnitude, which characterizes the long-term growth rate of infections. If $\widehat{\rho}(K) > 1$, each infected individual generates more than one secondary infection on average, leading to an epidemic outbreak. Conversely, if $\widehat{\rho}(K) < 1$, the infection chain eventually dies out. The Perron-Frobenius theorem [54, 55] guarantees that for a non-negative, irreducible matrix K, there is a unique largest eigenvalue $\widehat{\rho}(K)$. This eigenvalue is real and positive. In epidemiology, the largest eigenvalue governs the long-term behavior of the infection spread. The theorem also states that there exists a non-negative eigenvector associated with $\widehat{\rho}(K)$. This eigenvector represents the stable proportion of infections in each compartment over time. Geometrically, applying K iteratively to an initial infected population vector results in exponential growth proportional to $\widehat{\rho}(K)$. Thus, the spectral radius determines whether the epidemic grows or declines, making it the natural choice for $\mathcal{R}_0$. From the given system of

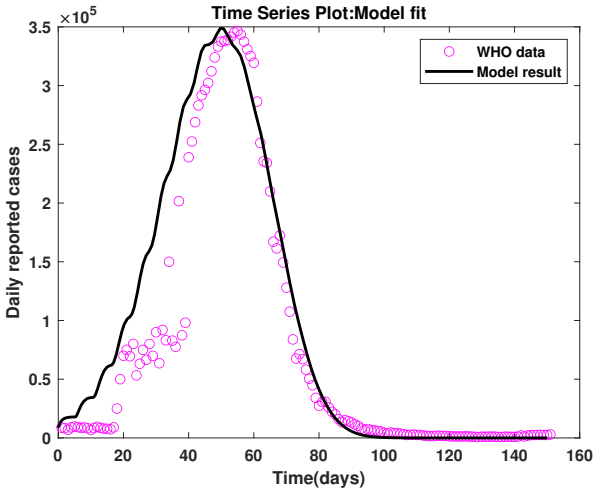

Figure 2. The trajectory of infected population, $I(t)$ of model (1), is fitted to real-time records of COVID-19 cases, during the third wave of COVID-19 in India, ensuring accurate alignment

equations in (1), the equation governing the infected population $I(t)$ is

$$\frac{dI}{dt} = \frac{\beta S(t-\tau_1)I(t-\tau_1)}{N} - (c+\rho_0)I(t).$$

In this equation, $\frac{\beta S(t-\tau_1)I(t-\tau_1)}{N}$ represents the new infections caused by interaction between susceptible $S(t)$ and infected $I(t)$ individuals, with transmission rate β. Here $(c+\rho_0)I(t)$ represents removal from the infected class due to recovery (with recovery rate c) and death (with infected death rate ρ_0). For the disease to be eradicated, $\frac{dI}{dt} < 0$. Here, linearizing at the disease-free steady state $\mathcal{E}_0$, we get $F = \frac{\beta S_0}{N_0}$, and $V = (c+\rho_0)$. Hence $K = FV^{-1} = \frac{\beta S_0}{N_0(c+\rho_0)}$. Thus, by substituting the value of S_0, we get the basic reproduction number for the model (1) as follows

$$\mathcal{R}_0 = \frac{\beta p((k+\rho)(r_1+\rho)(1-q)+kqr_1)}{N_0(c+\rho_0)(\mu(k+\rho)+\rho(r_1(\mu+\rho)+k(r_1+\rho)+\rho))} = \frac{\beta p\phi_3}{N_0\phi_1\eta_2}.$$

We deduce the endemic equilibrium of our model (1) as $\mathcal{E}_1 = (S_1, I_1, V_1, R_1, A_1)$ where,

$$S_1 = \frac{\mathcal{R}_0\phi_1}{p\phi_3}, \quad I_1 = \frac{N^*\eta_2\eta_4\phi_1(\mathcal{R}_0-1)}{\beta\phi_2\eta_3}, \quad V_1 = \frac{N^*\mu\eta_2+\beta pq}{\beta\eta_3}, \quad R_1 = \frac{N^*\eta_2\phi_1 c(\mathcal{R}_0-1)}{\beta\eta_3\phi_2},$$
$$A_1 = \frac{\beta p(c\eta_3 r_2(1-q)+kq\eta_2\eta_4)+N^*\eta_2(k\mu\eta_2\eta_4-c\eta_1\eta_3 r_2)}{\beta\eta_3\phi_2}. \tag{4}$$

It is clear from (4) that a unique positive endemic equilibrium only exists if $\mathcal{R}_0 > 1$. If $\mathcal{R}_0$ lies below 1, only the disease-free equilibrium is viable, and no biologically feasible endemic state exists. Consequently, we posit the following hypotheses based on Eq. (4):

H_1. In the case where $\mathcal{R}_0 < 1$, the only equilibrium point that exists is the infection-free equilibrium.

H_2. If $\mathcal{R}_0 > 1$, the system (1) admits two biologically feasible equilibrium points: The infection-free equilibrium $\mathcal{E}_0$ and the endemic equilibrium $\mathcal{E}_1$.

Table 1. Representation of parameters in model (1)

Parameters	Values	Source
τ_1	5.235	Estimated
τ_2	64.707193	Estimated
τ_3	60.61919	Estimated
q	0.174298	Estimated
β	2.09099	Estimated
μ	0.01076363	Estimated
r_1	0.024261	Estimated
c	0.93476	Estimated
k	0.0383658	Estimated
r_2	0.229543	Estimated
ρ	$\frac{1}{70\times365}$	[58]
p	$N(0)\times\rho$	-
ρ_0	0.09	Estimated
$N(0)$	1390537387	[58]

Data fitting and calibration of model parameters

This section presents a case study investigating the spread of COVID-19 in India, focusing on the daily increase in infected individuals. It utilizes the least squares curve fitting method to estimate parameters and validates theoretical findings with statistical data from India, sourced from references [56–58]. Our model (1) is fitted to daily data on COVID-19 cases in India from November 2021 to March 2022, which includes periods with numerous reinfection cases. Parameter estimation employs two approaches: initial net inflow rate and natural death rate sourced from reliable data [58], followed by determination of unknown parameters such as time-delay, disease mortality rate of infected individuals, and initial conditions through minimization of the sum of squared errors using collected data. The natural mortality rate is based on the average life expectancy of the Indian population (70 years), translating to a daily mortality rate of $\frac{1}{70\times365}$. The daily birth rate is calculated as the product of the initial total population and mortality rate, denoted as $p = N_0 \times \rho$. Remaining model parameters in (1) are derived from daily infected case data using statistical procedures in the R programming language's PBSddesolve package. Optimization employs the `Optim()` function to minimize the sum of squared errors, where the cost function is defined as $\text{Err} = \sum_{j=1}^{n}(\mathcal{X}(t_j) - \mathcal{Y}(t_j))^2$, with $\mathcal{Y}(t_j)$ representing daily reported cases and $\mathcal{X}(t_j)$ denoting the model solution (1) at time t_j. The estimated mortality rate of COVID-19-infected individuals exceeds the natural death rate of other compartments, consistent with real-world observations. Model fit to data Figure 2 demonstrates good alignment, with demographic parameters and initial values summarized in Table 1. The initial fully vaccinated population is set at 517,558,003 (as of November 13, 2021). Utilizing estimated parameters, the basic reproduction number $\mathcal{R}_0$ is determined to be 1.29661, exceeding the critical threshold of 1. Reference [49] notes an incubation period of 3 to 7 days, while [20] reports waning COVID-19 antibodies in 8 to 9 weeks. Achieving full vaccination in India typically requires 4 to 16 weeks, depending on vaccine types [50]. Consequently, our model estimates latent, vaccination, and susceptibility periods as approximately 5.235, 64.707193, and 60.61919 days, respectively, closely resembling real-world scenarios.

Time delay-free system dynamics: exploring parameter influences

To gain insights into the influence of system parameters apart from time delay, we analyze the dynamics of the system without any time delays. This approach enables us to study the effects of

various factors on the behavior of the system, excluding the influence of time delay.

Parameter sensitivity analysis

In existing studies, sensitivity analysis has been employed to determine the importance of various factors that influence disease transmission and prevalence. To mitigate disease spread, it is crucial to manage variations in the parameters of the proposed model to ensure $\mathcal{R}_0 < 1$. The sensitivity index of a variable relative to a parameter represents the ratio of their relative changes, calculated as shown in references [59, 60], $S[h] = \frac{h}{\mathcal{R}_0} \times \frac{\partial \mathcal{R}_0}{\partial h}$. This process involves the computation of normalized sensitivity indices for parameters identified previously. The sensitivity indices for parameters are presented in Table 2. These findings indicate that the disease transmission rate, β, emerges as the most sensitive parameter. Following β, the parameter r_1, which is the susceptibility rate of immune individuals, shows significant sensitivity. In contrast, the natural mortality rate, ρ, is identified as the least sensitive parameter within the system under study.

Table 2. Sensitivity indices of $\mathcal{R}_0$ with respect to system parameters

Parameters	Sensitivity Index	Parameters	Sensitivity Index
ρ	-0.999616	μ	-0.419536
ρ_0	-0.0878254	r_1	0.256718
q	-0.000458286	c	-0.912175
p	0	k	0.162434
β	1	r_2	0

Local stability analysis of the infection-free equilibrium

Theorem 2 *When we consider system (1) with no time-delay, the system's infection-free steady state $\mathcal{E}_0$ exhibits local asymptotic stable behaviour (instability) if $\mathcal{R}_0 < 1$ ($\mathcal{R}_0 > 1$).*

Proof

We first derive the following linearized matrix evaluated at any arbitrary equilibrium point, $\mathcal{E}^*$, for model (1) without time-delays

$$\mathcal{J} = \begin{pmatrix} -\eta_1 - \frac{\beta I^*}{N^*} & -\frac{\beta S^*}{N^*} & 0 & 0 & r_1 \\ \frac{\beta I^*}{N^*} & -\eta_2 + \frac{\beta S^*}{N^*} & 0 & 0 & 0 \\ \mu & 0 & -\eta_3 & 0 & 0 \\ 0 & c & 0 & -\eta_4 & 0 \\ 0 & 0 & k & r_2 & -\eta_5 \end{pmatrix}. \tag{5}$$

The above matrix, when evaluated at the infection-free equilibrium ($\mathcal{E}_0$), possesses the following characteristic equation

$$(\beta S_0 - \lambda N_0 - N_0\eta_2)(\eta_4 + \lambda)(\lambda^3 + \lambda^2(\eta_1 + \eta_3 + \eta_5) + \lambda(\eta_1\eta_3 + \eta_1\eta_5 + \eta_3\eta_5) + \phi_1) = 0.$$

The above polynomial possess the eigenvalues $\lambda_1 = -\eta_1$, $\lambda_2 = \eta_2(\mathcal{R}_0 - 1)$ and the remaining are the roots of the following cubic polynomial

$$\lambda^3 + \lambda^2(\eta_1 + \eta_3 + \eta_5) + \lambda(\eta_1\eta_3 + \eta_1\eta_5 + \eta_3\eta_5) + \phi_1 = 0. \tag{6}$$

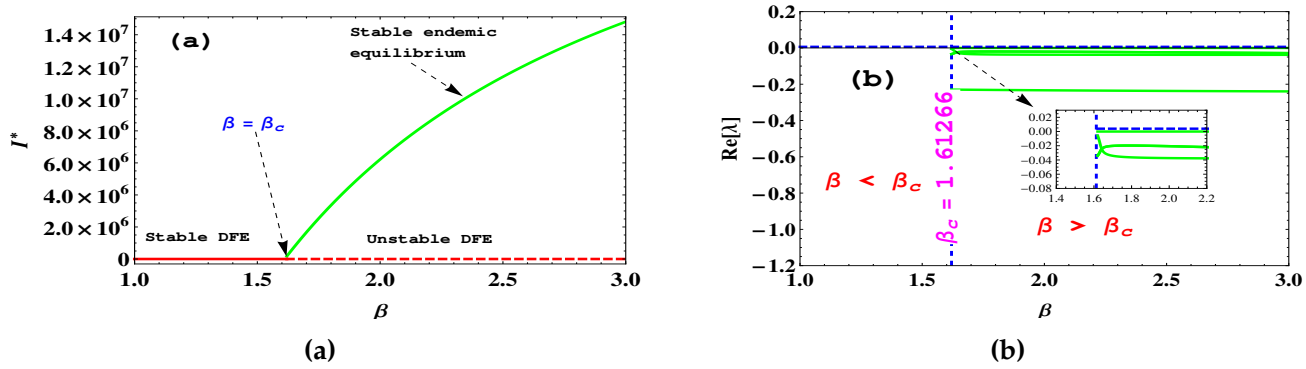

Figure 3. Figure (a) shows the occurrence of forward bifurcation with respect to β. The solid red line indicates $\mathcal{E}_0$ is stable for $\beta < \beta_c$, whereas in the region $\beta > \beta_c$, $\mathcal{E}_0$ becomes unstable (red-dashed lines) and $\mathcal{E}_1$ exists and is stable (green solid line). Figure (b) represents the plot of the real part of eigenvalues associated with the steady state $\mathcal{E}_1$ and the bifurcation parameter, β

As per the Routh-Hurwitz criteria for the polynomial $\lambda^3 + a_1\lambda^2 + a_2\lambda^2 + a_3 = 0$, the Eq. (6) possess roots with negative real parts, since $a_1 = \eta_1 + \eta_3 + \eta_5 > 0$, $a_2 = \eta_1\eta_3 + \eta_1\eta_5 + \eta_3\eta_5 > 0$, $a_3 = \phi_1 > 0$ and $a_1a_2 - a_3 = \eta_1^2(\eta_3 + \eta_5) + \eta_3^2(\eta_1 + \eta_5) + \eta_5^2(\eta_1 + \eta_3) + 2\eta_1\eta_3\eta_5 + k\mu r_1 > 0$. Thus, the infection-free steady state state is locally asymptotically stable for $\mathcal{R}_0 < 1$ and it becomes unstable for $\mathcal{R}_0 > 1$ since both depends on the sign of $\lambda_2 = \eta_2(\mathcal{R}_0 - 1)$. □

Local stability analysis of endemic equilibrium

Due to the complex nature of the eigenvalues associated with the Jacobian matrix evaluated at the endemic steady state $\mathcal{E}_1$, they are not explicitly presented. Instead, we have computed the eigenvalues for the steady state $\mathcal{E}_1$, and their respective stability regions are depicted in Figure 3a and Figure 3b. In the absence of delays, we identify the disease transmission rate linked to primary infections (β) as the bifurcation parameter, given its pivotal role in infection dynamics.
It is observed that at higher values of β (for $\beta > \beta_c$), the endemic equilibrium exhibits stability, while the infection-free equilibrium becomes unstable. This indicates that an increase in the disease transmission rate prolongs the persistence of the disease in the human population, making eradication unachievable. These scenarios are illustrated in Figure 3a and Figure 3b, respectively. Figure 3a clearly demonstrates that when $\mathcal{R}_0 > 1$ ($\beta > \beta_c$), the infection-free equilibrium loses stability, giving rise to a stable endemic equilibrium. This reflects a forward bifurcation in the system, as the steady state $\mathcal{E}_1$ exists only when $\mathcal{R}_0 > 1$, bifurcating from $\mathcal{E}_0$ at $\mathcal{R}_0 = 1$ ($\beta = \beta_c$). The critical value for the bifurcation parameter β is approximately 1.61266. To further elucidate the stable nature of the endemic steady state, we have plotted the real parts of all eigenvalues concerning the bifurcation parameter β in Figure 3b. As evident from Figure 3b, the real parts of all characteristic values associated with $\mathcal{E}_1$ lie below the line $Re(\lambda) = 0$ (as each eigenvalue possesses a negative real part), indicating the stable nature of the endemic steady state $\mathcal{E}_1$ in the $\beta > \beta_c$ regime.

System dynamics with time delays

In this section, we learn more about how time de lays affect a system's behavior and changes over time. The investigation of delay-induced bifurcations carries significant implications in the field of epidemiology, enabling the prediction of intervention effectiveness and enhancing our understanding of the circumstances that lead to disease eradication or sustained endemicity. Within this section, we conduct an analysis to determine the stability of equilibria and the conditions necessary for the occurrence of Hopf bifurcation, by employing time delay as the parameter for

bifurcation.

The objective is to examine the stability of the developed model and analyze the occurrence of Hopf bifurcation. Let $\mathcal{E}^*(S^*, I^*, V^*, R^*, A^*)$ denote an arbitrary steady state of the model (1). Subsequently, we derive the linearized matrix evaluated at $\mathcal{E}^*$ for the delayed model (1) as follows.

$$\mathcal{J}_\tau = \begin{pmatrix} -\rho - \frac{\beta I^* e^{-\lambda\tau_1}}{N^*} - \mu e^{-\lambda\tau_2} & -\frac{\beta S^* e^{-\lambda\tau_1}}{N^*} & 0 & 0 & r_1 e^{-\lambda\tau_3} \\ \frac{\beta I^* e^{-\lambda\tau_1}}{N^*} & -\eta_2 + \frac{\beta S^* e^{-\lambda\tau_1}}{N^*} & 0 & 0 & 0 \\ \mu e^{-\lambda\tau_2} & 0 & -\eta_3 & 0 & 0 \\ 0 & c & 0 & -\eta_4 & 0 \\ 0 & 0 & k & r_2 & -\rho - r_1 e^{-\lambda\tau_3} \end{pmatrix}. \tag{7}$$

The above matrix (7) has the following characteristic equation

$$\left.\begin{array}{c} \lambda^5 + A_{11}\lambda^4 + A_{12}\lambda^3 + A_{13}\lambda^2 + A_{14}\lambda + A_{15} + e^{-\lambda\tau_1}\left(B_{11}\lambda^4 + B_{12}\lambda^3 + B_{13}\lambda^2 + B_{14}\lambda + B_{15}\right) \\ + e^{-\lambda_2}\left(E_{11}\lambda^4 + E_{12}\lambda^3 + E_{13}\lambda^2 + E_{14}\lambda + E_{15}\right) + e^{-\lambda\tau_3}\left(F_{11}\lambda^4 + F_{12}\lambda^3 + F_{13}\lambda^2 + F_{14}\lambda + F_{15}\right) \\ + e^{-\lambda(\tau_1+\tau_2)}\left(G_{11}\lambda^3 + G_{12}\lambda^2 + G_{13}\lambda + G_{14}\right) + e^{-\lambda(\tau_1+\tau_3)}\left(H_{11}\lambda^3 + H_{12}\lambda^2 + H_{13}\lambda + H_{14}\right) \\ + e^{-\lambda(\tau_2+\tau_3)}\left(K_{11}\lambda^3 + K_{12}\lambda^2 + K_{13}\lambda + K_{14}\right) + e^{-\lambda(\tau_1+\tau_2+\tau_3)}\left(L_{11}\lambda^2 + L_{12}\lambda + L_{13}\right) \end{array}\right\} = 0, \tag{8}$$

where, A_{1i}, B_{1i}, E_{1i}, F_{1i}, G_{1j}, H_{1j}, K_{1j} for $i = 1,2,3,4,5$, $j = 1,2,3,4$ and L_{1l} for $l = 1,2,3$ are given in Appendix A.

Theorem 3 *For any arbitrary steady state $\mathcal{E}^*(S^*, I^*, V^*, R^*, A^*)$ of model (1), we have the following results*

(a) In the case of system (1), where $\tau_1 > 0$ and $\tau_2 = \tau_3 = 0$, the equilibrium of (1) exhibits local asymptotic stability within the interval (0,τ_{10}). Additionally, a Hopf bifurcation arises specifically when τ_1=τ_{10}.

(b) In the case of system (1), where $\tau_2 > 0$ and $\tau_1 = \tau_3 = 0$, the equilibrium of (1) exhibits local asymptotic stability within the range of $\tau_2 \in (0, \tau_{20})$. Additionally, a Hopf bifurcation arises when $\tau_2 = \tau_{20}$.

(c) In the case of system (1), where $\tau_3 > 0$ and $\tau_1 = \tau_2 = 0$, the equilibrium of (1) is locally asymptotically stable within the range of $\tau_3 \in (0, \tau_{30})$ where $\tau_{30} = \min\left\{\tau_{3i}^{(0)}\right\}$, $\quad i = 1,2,\ldots 5$. Further the system (1), undergoes a Hopf bifurcation when $\tau_3 = \tau_{30}$.

(d) The equilibrium $\mathcal{E}^*$ of system (1) exhibits local asymptotic stability within the parameter ranges (0, τ_1^*), (0, τ_{20}), and (0, τ_{30}). Additionally, when τ_1=τ_1^*, the system (1) undergoes a Hopf bifurcation at $\mathcal{E}^*$.

(e) The equilibrium $\mathcal{E}^*$ of system (1) exhibits local asymptotic stability within the parameter ranges (0, τ_{10}), (0, τ_2^*), and (0, τ_{30}). Additionally, when τ_2=τ_2^*, the system (1) undergoes a Hopf bifurcation at $\mathcal{E}^*$.

(f) The equilibrium state $\mathcal{E}^*$ of system (1) exhibits local asymptotic stability within the parameter ranges (0, τ_{10}), (0, τ_{20}), and (0, τ_3^*). Additionally, when τ_3=τ_3^*, the system (1) undergoes a Hopf bifurcation at $\mathcal{E}^*$.

Remark 1 *For the proof of Theorem 3$(a)-(f)$, the readers may refer to Appendix B.*

4 Numerical results and analysis: insights from estimated parameters

Based on the variables calibrated, the estimated basic reproduction ratio is approximately 1.29661, signifying that the population was persistently in an endemic state throughout the observed period. Subsequent calculations lead us to the disease equilibrium $\mathcal{E}_1(621.985, 7.45156, 174.478, 29.9892, 559.152) \times 10^6$ for system (1).

Comprehensive analysis under various scenarios

Understanding disease control with latency period

The initial scenario contemplates a population receiving a single vaccine dose, with previously protected individuals becoming susceptible again instantaneously. Additionally, a latency period precedes the manifestation of infectiousness in infected individuals. This scenario is modeled by setting τ_2 and τ_3 to zero and assigning a positive value to τ_1 in differential Eq. (1). Utilizing MATLAB for this analysis, we calculate a unique positive root θ_{10} in Eq. (B.3), identified as $m_{10} = 0.001615$. The values of θ_{10} and τ_{10} are found to be 0.041305 and 29.437, respectively. Verifying $Y_{11}Y_{13} + Y_{12}Y_{14} = 0.00003855 > 0$ confirms that the necessary conditions for a Hopf bifurcation are met. Numerical simulations illustrated in Figure 4 depict the endemic equilibrium $\mathcal{E}_1$ behavior for varying τ_1. Selecting $\tau_1 = 29$ results in a locally asymptotically stable endemic equilibrium as shown in Figure 4b, suggesting effective disease control under this scenario. However, setting $\tau_1 = 30$ destabilizes the endemic equilibrium, triggering a periodic behavior as shown in Figure 4a. Notably, we find that the disease cannot be controlled only in the presence of a latent period delay, specifically, when the average latency period of an individual exceeds approximately thirty days.

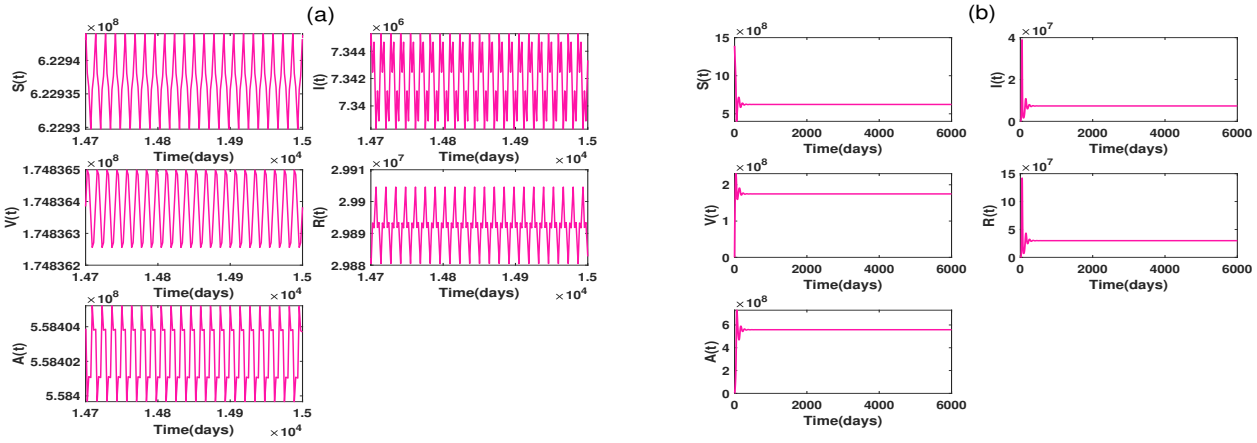

(a) **(b)**

Figure 4. For case (a) of Theorem 3, Figure (a) shows the periodic oscillations of solution trajectories for $\tau_1 = 30 > \tau_{10}$ in which the steady state $\mathcal{E}_1$ is unstable. Conversely Figure (b) shows that the steady state $\mathcal{E}_1$ is stable for $\tau_1 = 29 < \tau_{10}$

Exploring scenarios with immediate symptoms and vaccination delay

Another scenario examined involves immediate symptom onset and infectiousness post-infection and instant susceptibility reinstatement post-antibody protection. This scenario introduces a delay in administering the required vaccine doses, represented by setting τ_1 and τ_3 to zero, while τ_2 is assigned a value greater than zero. Employing similar analytical methods, we determine the critical value τ_{20} to be 14.2345. Numerical simulations for varying τ_2 values as shown in Figure 5 reveal that the disease equilibrium $\mathcal{E}_1$ remains locally asymptotically stable for $\tau_2 = 14$. However, for $\tau_2 > 14.2345$ as shown in Figure 5a, the equilibrium becomes unstable with solutions deviating from the steady state $\mathcal{E}_1$. This scenario reflects the practical challenges of adhering to tight vaccination schedules, emphasizing the significance of considering realistic vaccination delays in disease control strategies.

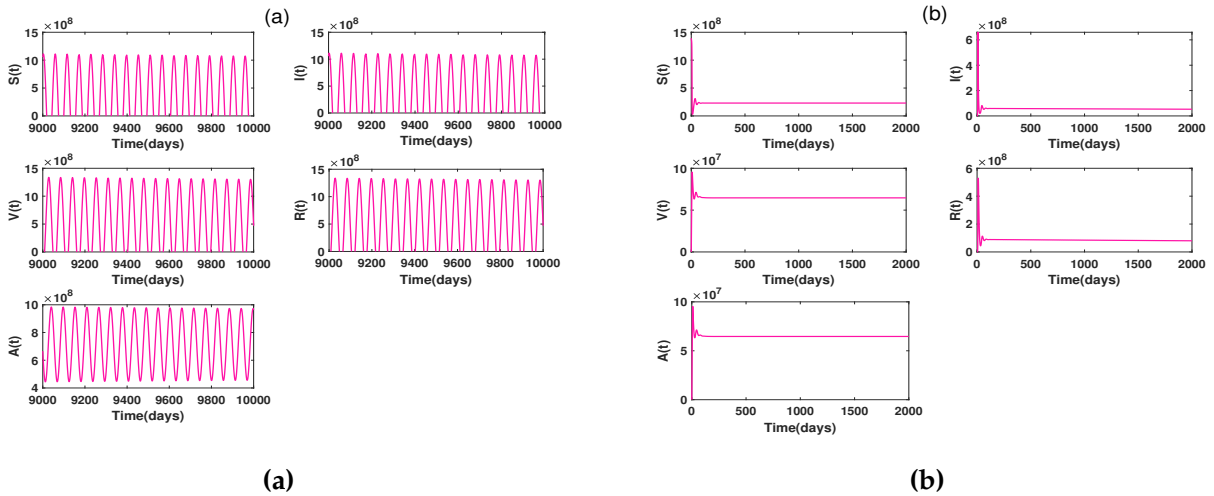

(a) **(b)**

Figure 5. For case (b) of Theorem 3, Figure (a) shows the periodic oscillations of solution trajectories for $\tau_2 = 14.39 > \tau_{20}$ in which the steady state $\mathcal{E}_1$ is unstable. Conversely Figure (b) shows that the steady state $\mathcal{E}_1$ is stable for $\tau_2 = 14 < \tau_{20}$

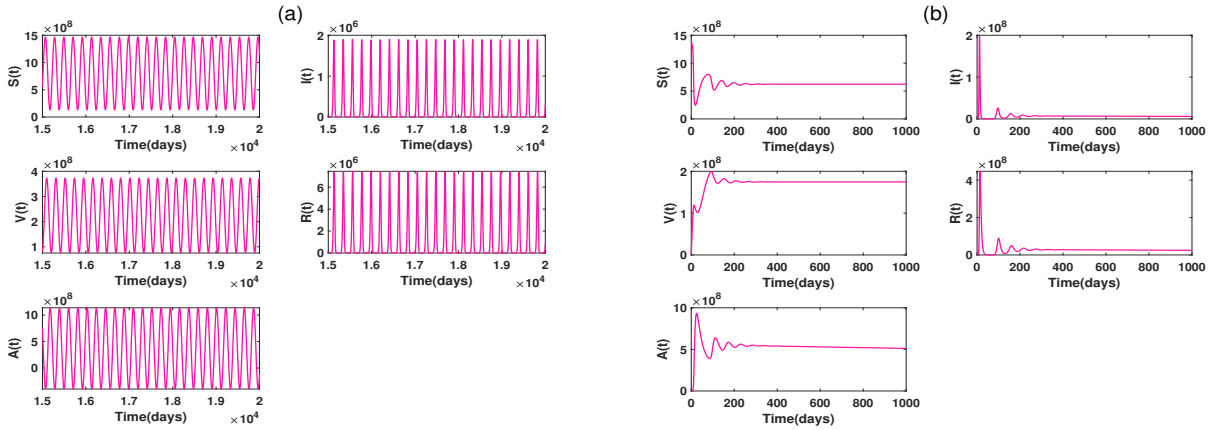

(a) **(b)**

Figure 6. For case (c) of Theorem 3, Figure (a) shows the periodic oscillations of solution trajectories for $\tau_3 = 54 > \tau_{30}$ in which the steady state $\mathcal{E}_1$ is unstable. Conversely Figure (b) shows that the steady state $\mathcal{E}_1$ is stable for $\tau_3 = 52 < \tau_{30}$

Investigating the role of susceptibility period on disease control and immunity

In a different scenario, individuals are immunized against the disease, but there is a period before they become susceptible again, and the time periods associated with latency and achieving full vaccination are nonexistent. The duration of antibody protection, or the susceptibility period, is pivotal for understanding disease dynamics. Figure 6 plots solution trajectories for various τ_3 values, identifying a critical threshold of approximately 53.386 for τ_3. When this average delay in losing antibodies exceeds approximately 53 days, a significant change occurs in the disease dynamics. This change is marked by the deviation from the endemic equilibrium and the occurrence of a Hopf bifurcation, which is clearly shown in Figure 6a and Figure 6b. The Hopf bifurcation observed in our simulations indicates that, beyond the critical value of τ_3, the disease tends to exhibit periodic resurgences in the population. This means that after a specific time period, infected individuals become susceptible again due to the loss of antibodies, leading to a revival of the disease. These periodic fluctuations in the disease prevalence can have significant implications

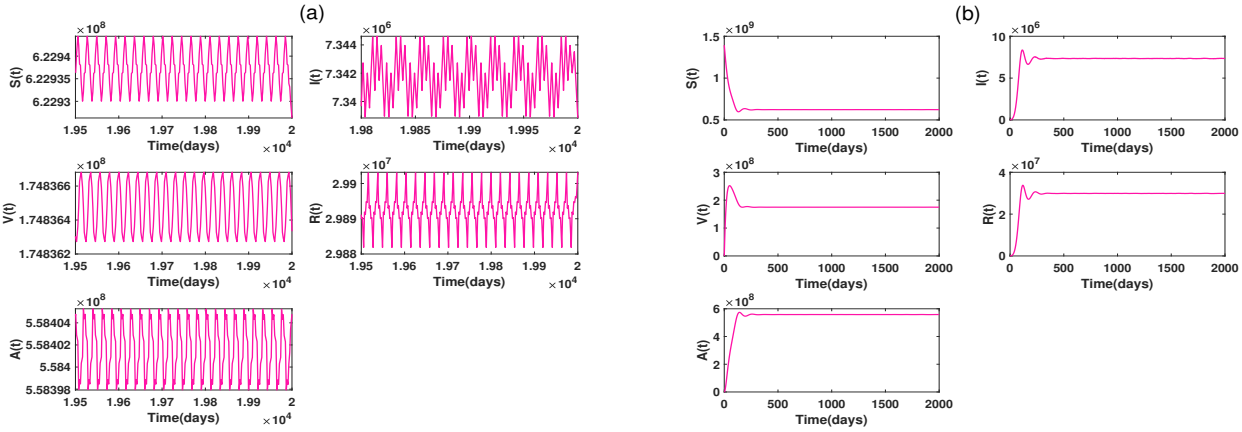

(a) **(b)**

Figure 7. For case (d) of Theorem 3, Figure (a) shows the periodic oscillations of solution trajectories for $\tau_1 = 40 > \tau_1^*$ in which the steady state $\mathcal{E}_1$ is unstable. Conversely Figure (b) shows that the steady state $\mathcal{E}_1$ is stable for $\tau_1 = 38 < \tau_1^*$

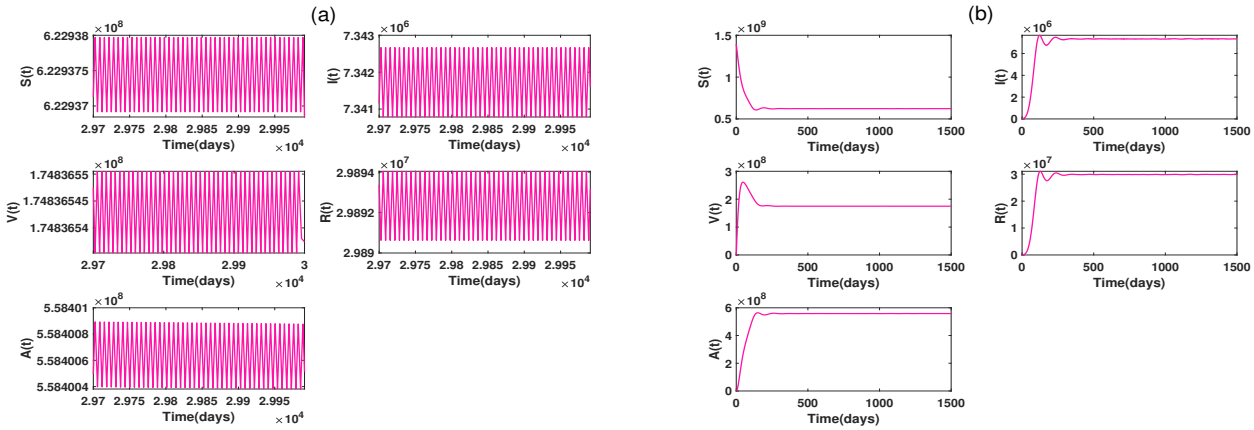

(a) **(b)**

Figure 8. For case (e) of Theorem 3, Figure (a) shows the periodic oscillations of solution trajectories for $\tau_2 = 12 > \tau_2^*$ in which the steady state $\mathcal{E}_1$ is unstable. Conversely Figure (b) shows that the steady state $\mathcal{E}_1$ is stable for $\tau_2 = 10 < \tau_2^*$

for public health and disease control strategies. The findings from our simulations suggest that the duration of antibody protection (susceptibility period) is crucial for understanding disease dynamics. Suppose the average time period for antibodies to vanish exceeds the critical value, there is a risk of periodic outbreaks, which may lead to challenges in disease control and require appropriate public health responses.

System dynamics with multiple time-delays

Lastly, we consider a situation with all three delays: the latent period delay, the vaccination delay, and the susceptibility period delay. By performing simulations under different conditions, we identify critical values for each delay. We perform numerical simulations and predict the dynamics under the following situations

Initially, our focus shifts to a configuration where the vaccination delay is set to 10 days, complemented by a susceptibility period delay of 51 days, both calibrated within their respective ranges

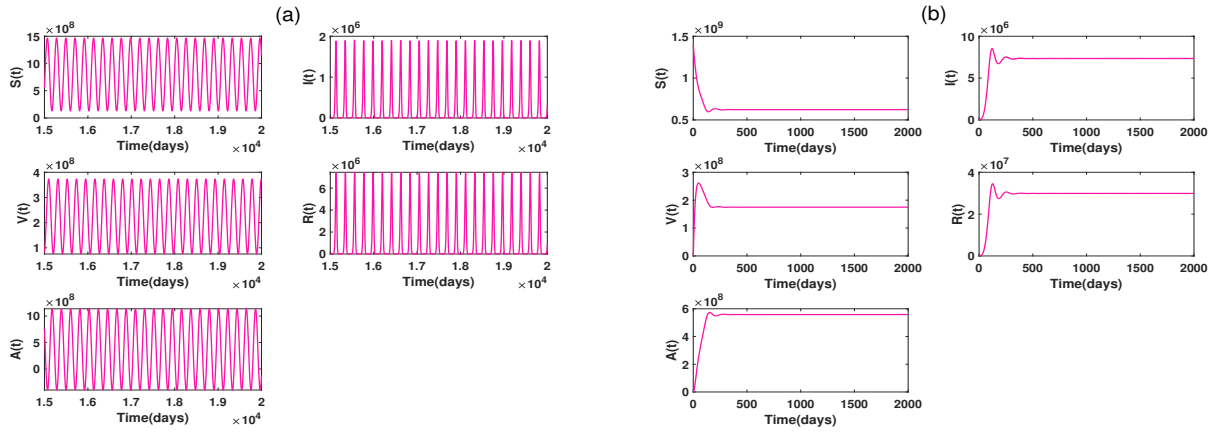

(a) **(b)**

Figure 9. For case (f) of Theorem 3, Figure (a) shows the periodic oscillations of solution trajectories for $\tau_3 = 51 > \tau_3^*$ in which the steady state $\mathcal{E}_1$ is unstable. Conversely Figure (b) shows that the steady state $\mathcal{E}_1$ is stable for $\tau_3 = 49 < \tau_3^*$

conducive to stability. The critical discovery in this setup is the identification of the vital latency period threshold, calculated to be approximately 39.2385 days. This threshold delineates a fine balance; should the actual latency period be shorter, say less than a month, the disease's presence in the population remains steady and stable. Conversely, extending this period to around 40 days disrupts this equilibrium, resulting in a heightened risk of outbreak escalations. The simulations, as depicted in Figure 7a and Figure 7b, visually articulate these findings.

Expanding our exploration, two additional scenarios were meticulously analyzed. In the first, the latency period was adjusted to 25 days (positioned safely within its stability realm) and the susceptibility period to 51 days (again, within a stable domain), while introducing a non-zero vaccination delay. This analysis unearthed a critical vaccination delay threshold of approximately 11.2893 days. The second scenario maintained the latency period at 25 days and the vaccination delay at a manageable 10 days, aiming to pinpoint the critical threshold for the susceptibility period delay, which was found to be roughly 50.1086 days. The graphical representations of these results are visually captured in Figure 8a, Figure 8b and Figure 9a, Figure 9b.

Furthermore, the phase portrait diagram corresponding to each case as presented in Theorem 3 and depicted in Figure 10, Figure 11 and Figure 12, offers a visual representation of the unstable equilibrium of the system in these circumstances.

5 Results and discussion

This article presents an epidemic model incorporating multiple time delays and emphasizes several key concepts:

- We have created a separate compartment for individuals with immunity, either post-recovery or through vaccination, with a significant time delay (τ_3) representing the susceptibility period for these immune individuals. This acknowledges that disease persistence can occur when immunity fades or when there are variations in the time delay of susceptibility.
- The model guarantees that all solutions remain positive and constrained within biologically feasible limits, ensuring the validity of the system in representing real-world epidemiological dynamics. Additionally, the solutions of the considered model are proven to be bounded, confirming the applicability of the model over the long term.
- The disease-free equilibrium (DFE) is determined, representing a state where the infection

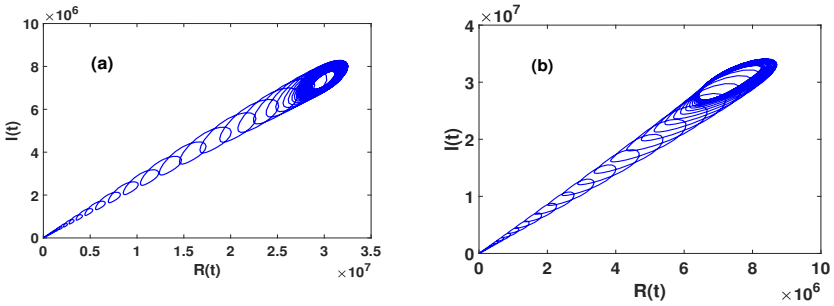

Figure 10. In Figure (a), the phase portrait diagram illustrates the unstable phase for Case (a) as outlined in Theorem 3, where $\tau_1 = 30 > \tau_{10}$. In Figure (b), the diagram presents the unstable phase for Case (d) from Theorem 3, where $\tau_1 = 40 > \tau_1^*$, while τ_2 and τ_3 remain below τ_{20} and τ_{30}, respectively

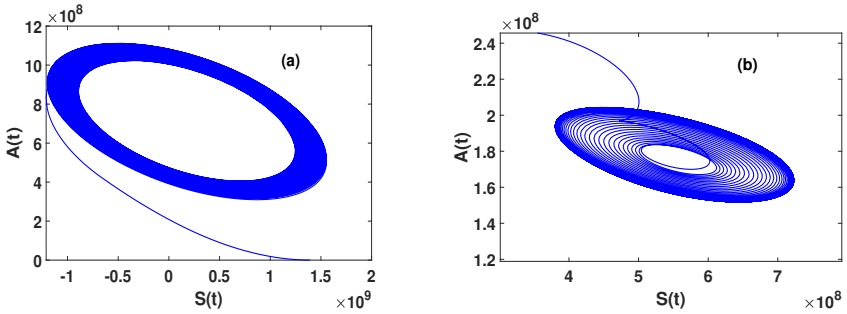

Figure 11. In Figure (a), the phase portrait diagram illustrates the unstable phase for Case (b) as outlined in Theorem 3, where $\tau_2 = 14.39 > \tau_{20}$. In Figure (b), the diagram presents the unstable phase for Case (e) from Theorem 3, where $\tau_2 = 12 > \tau_2^*$, while τ_1 and τ_3 remain below τ_{10} and τ_{30}, respectively

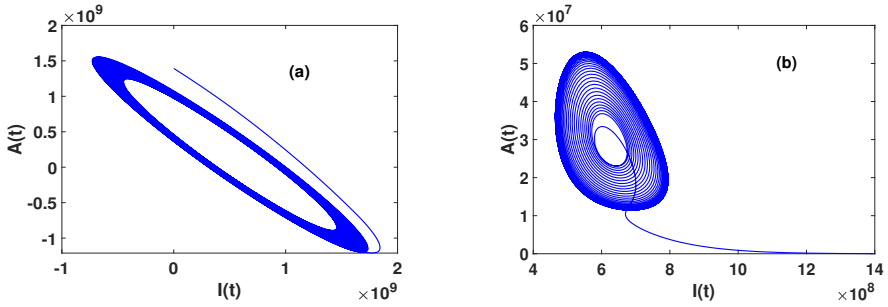

Figure 12. In Figure (a), the phase portrait diagram illustrates the unstable phase for Case (c) as outlined in Theorem 3, where τ_3=54 $> \tau_{30}$. In Figure (b), the diagram presents the unstable phase for Case (e) from Theorem 3, where $\tau_3 = 51 > \tau_3^*$, while τ_1 and τ_2 remain below τ_{10} and τ_{20}, respectively

is eliminated over time. Additionally, the endemic equilibrium is derived, corresponding to a scenario in which the disease remains within the population. The basic reproduction number ($\mathcal{R}_0$) is calculated using the next-generation matrix method, and it serves as a threshold parameter that determines whether the infection will persist or decline.

- Sensitivity analysis is conducted to evaluate the impact of system parameters on the basic reproduction number ($\mathcal{R}_0$). The results indicate that the disease transmission rate (β) exhibits the highest sensitivity, followed by the susceptibility rate of immune individuals (r_1). In contrast, the mortality rate (ρ_0) has a negligible effect on disease transmission, suggesting that intervention strategies should prioritize reducing β rather than modifying natural death rates.
- For $\mathcal{R}_0 < 1$, the disease-free equilibrium is locally stable, which indicates that the infection will diminish over time. Conversely, when $\mathcal{R}_0 > 1$, the disease-free equilibrium loses its stability, and leads to the existence of a stable endemic equilibrium, which denotes disease persistence. The stability conditions are further verified by plotting the real parts of the eigenvalues

corresponding to the linearized matrix evaluated at the steady state $\mathcal{E}_1$.

- The system exhibits forward bifurcation, indicating a continuous transition from a disease-free equilibrium to an endemic state as the transmission rate (β) exceeds a critical threshold. The Hopf bifurcation analysis demonstrates that time delays associated with immunity loss and reinfection can induce periodic outbreaks, resulting in oscillatory fluctuations in disease prevalence.
- Numerical simulations support the theoretical findings by demonstrating the effects of time delays, vaccination rates, and immunity loss on disease transmission dynamics. The results indicate that minimizing time delays and enhancing immunity through vaccination can effectively reduce the risk of outbreaks. The parameters of the model are calibrated using real-time COVID-19 data to ensure consistency with observed epidemiological trends. Furthermore, the identification of critical delay thresholds provides valuable insights into the transmission dynamics of the disease.
- The findings of this study demonstrate that a shorter duration of immunity in individuals increases the likelihood of periodic outbreaks, highlighting the importance of implementing booster vaccination programs. Furthermore, timely interventions in vaccination and reinfection prevention are essential for mitigating the risk of recurring disease resurgences.
- One potential limitation of the current study is that the mathematical model has been analyzed in the integer-order case with constant time delays. While this approach provides valuable insights into the stability and bifurcation analysis of the considered system, there are opportunities for further refinement. A promising direction for future research is to extend the model to a fractional-order model, which can account for the long-term memory and hereditary properties of immune responses. Additionally, incorporating time-varying parameters and delays would provide a more realistic representation of immunity dynamics due to factors such as waning antibody protection, evolving pathogen characteristics, or interventions.

Appendix A

$$A_{11} = 2\rho + \eta_2 + \eta_3 + \eta_4, \quad A_{12} = \rho^2 + (2\eta_2 + 2\eta_3 + 2\eta_4)d + \eta_2(\eta_3 + \eta_4) + \eta_3\eta_4,$$
$$A_{13} = (\eta_2 + \eta_3 + \eta_4)\rho^2 + 2\rho(\eta_2(\eta_3 + \eta_4) + \eta_3\eta_4) + \eta_2\eta_3\eta_4, \quad A_{14} = \rho(2\eta_2\eta_3\eta_4 + \rho(\eta_3\eta_4 + \eta_2(\eta_3 + \eta_4))),$$
$$A_{15} = \rho^2\eta_2\eta_3\eta_4, \quad B_{11} = \frac{1}{N^*}\beta(I^* - S^*), \quad B_{12} = \frac{1}{N^*}(\beta(\rho + \eta_2 + \eta_3 + \eta_4)I^* - \beta S^*(2\rho + \eta_3 + \eta_4)),$$
$$B_{13} = \frac{1}{N^*}(\beta I^*(\eta_2\eta_4 + \eta_3(\eta_2 + \eta_4) + \rho(\eta_2 + \eta_3 + \eta_4)) - \beta S^*(\rho^2 + (2\eta_3 + 2\eta_4)\rho + \eta_3\eta_4)),$$
$$B_{14} = \frac{1}{N^*}\beta(I^*\eta_2\eta_3\eta_4 + \rho(I^*\eta_2\eta_4 + \eta_3(I^*\eta_2 - \eta_4(2S^* - I^*))) - \rho^2 S^*(\eta_3 + \eta_4)), \quad B_{15} = \frac{1}{N^*}\beta\rho\eta_3\eta_4(\eta_2 I^* - \rho S^*),$$
$$E_{11} = \mu, \quad E_{12} = \mu(\rho + \eta_2 + \eta_3 + \eta_4), \quad E_{13} = \mu(\rho\eta_4 + \eta_3(\rho + \eta_4) + \eta_2(\rho + \eta_3 + \eta_4)),$$
$$E_{14} = \mu(\rho\eta_3\eta_4 + \eta_2(\rho\eta_4 + \eta_3(\rho + \eta_4))), \quad E_{15} = \rho\mu\eta_2\eta_3\eta_4, \quad F_{11} = r_1, \quad F_{12} = r_1(\rho + \eta_2 + \eta_3 + \eta_4),$$
$$F_{13} = r_1(\rho\eta_4 + \eta_3(\rho + \eta_4) + \eta_2(\rho + \eta_3 + \eta_4)), \quad F_{14} = r_1(\rho\eta_3\eta_4 + \eta_2(\rho\eta_4 + \eta_3(\rho + \eta_4))), \quad F_{15} = \rho\eta_2\eta_3\eta_4 r_1,$$
$$G_{11} = -\frac{1}{N^*}\beta\mu S^*, \quad G_{12} = -\frac{1}{N^*}\beta\mu S^*(\rho + \eta_3 + \eta_4), \quad G_{13} = -\frac{1}{N^*}\beta\mu S^*(\rho\eta_4 + \eta_3(\rho + \eta_4)),$$
$$G_{14} = -\frac{1}{N^*}\beta\rho\mu S^*\eta_3\eta_4, \quad H_{11} = \frac{1}{N^*}\beta(I^* - S^* r_1), \quad H_{12} = \frac{1}{N^*}\beta r_1(I^*(\eta_2 + \eta_3 + \eta_4) - S^*(\rho + \eta_3 + \eta_4)),$$
$$H_{13} = -\frac{1}{N^*}\beta((((S^* - I^*)\eta_4 + \rho S^* - I^*\eta_2)\eta_3 + \eta_4(\rho S^* - \eta_2 I^*))r_1 + cI^* r_2),$$
$$H_{14} = \frac{1}{N^*}\beta\eta_3 r_1(\eta_2\eta_4 I^* - cI^* r_2 - \rho S^*\eta_4), \quad K_{11} = \mu r_1, \quad K_{12} = -\mu((\eta_2 + \eta_3 + \eta_4)r_1 - k),$$
$$K_{13} = \mu r_1(\eta_4(\eta_3 - k) + \eta_2(\eta_3 + \eta_4 - k)), \quad K_{14} = \mu\eta_2\eta_4 r_1(\eta_3 - k), \quad L_{11} = -\frac{1}{N^*}\beta\mu S^* r_1,$$
$$L_{12} = \frac{1}{N^*}\beta\mu S^* r_1(k - \eta_3 - \eta_4), \quad L_{13} = \frac{1}{N^*}\beta\mu S^*\eta_4 r_1(k - \eta_3).$$

Appendix B

Proof of Theorem 3(a) Suppose $\tau_1 > 0$, $\tau_2 = \tau_3 = 0$, the characteristic Eq. (8) becomes

$$\lambda^5 + \widetilde{\mathcal{B}}_1\lambda^4 + \widetilde{\mathcal{B}}_2\lambda^3 + \widetilde{\mathcal{B}}_3\lambda^2 + \widetilde{\mathcal{B}}_4\lambda + \widetilde{\mathcal{B}}_5 + e^{-\lambda\tau_1}(\widetilde{\mathcal{B}}_6\lambda^4 + \widetilde{\mathcal{B}}_7\lambda^3 + \widetilde{\mathcal{B}}_8\lambda^2 + \widetilde{\mathcal{B}}_9\lambda + \widetilde{\mathcal{B}}_0) = 0, \tag{B.1}$$

where $\widetilde{\mathcal{B}}_1 = A_{11} + E_{11} + F_{11}$, $\widetilde{\mathcal{B}}_2 = A_{12} + E_{12} + F_{12} + K_{11}$, $\widetilde{\mathcal{B}}_3 = A_{13} + E_{13} + F_{13} + k_{12}$, $\widetilde{\mathcal{B}}_4 = A_{14} + E_{14} + F_{14} + k_{13}$, $\widetilde{\mathcal{B}}_5 = A_{15} + E_{15} + F_{15} + k_{14}$, $\widetilde{\mathcal{B}}_6 = B_{11}$, $\widetilde{\mathcal{B}}_7 = B_{12} + G_{11} + H_{11}$, $\widetilde{\mathcal{B}}_8 = B_{13} + G_{12} + H_{12} + L_{11}$, $\widetilde{\mathcal{B}}_9 = B_{14} + G_{13} + H_{13} + L_{12}$, $\widetilde{\mathcal{B}}_0 = B_{15} + G_{14} + H_{14} + L_{13}$. Let $\lambda = i\theta_1$ ($\theta_1 > 0$) be root of Eq. (B.1) then, we have $N_{11}(\theta_1)\cos\tau_1\theta_1 + N_{12}(\theta_1)\sin\tau_1\theta_1 = N_{13}(\theta_1)$, and $N_{12}(\theta_1)\cos\tau_1\theta_1 - N_{11}(\theta_1)\sin\tau_1\theta_1 = N_{14}(\theta_1)$, where, $N_{11}(\theta_1) = \widetilde{\mathcal{B}}_6\theta_1^4 - \widetilde{\mathcal{B}}_8\theta_1^2 + \widetilde{\mathcal{B}}_0$, $N_{12}(\theta_1) = \widetilde{\mathcal{B}}_9\theta_1 - \widetilde{\mathcal{B}}_7\theta_1^3$, $N_{13}(\theta_1) = \widetilde{\mathcal{B}}_3\theta_1^2 - \widetilde{\mathcal{B}}_5 - \widetilde{\mathcal{B}}_1\theta_1^4$, $N_{14}(\theta_1) = \widetilde{\mathcal{B}}_2\theta_1^3 - \widetilde{\mathcal{B}}_4\theta_1 - \theta_1^5$. Here, $N_{13}^2(\theta_1) + N_{14}^2(\theta_1) = N_{11}^2(\theta_1) + N_{12}^2(\theta_1)$ from which, we get the following

$$\theta_1^{10} + \sigma_{11}\theta_1^8 + \sigma_{12}\theta_1^6 + \sigma_{13}\theta_1^4 + \sigma_{14}\theta_1^2 + \sigma_{15} = 0, \tag{B.2}$$

where $\sigma_{11} = \widetilde{\mathcal{B}}_1^2 - \widetilde{\mathcal{B}}_6^2 - 2\widetilde{\mathcal{B}}_2$, $\sigma_{12} = -2\widetilde{\mathcal{B}}_1\widetilde{\mathcal{B}}_3 + \widetilde{\mathcal{B}}_2^2 + 2\widetilde{\mathcal{B}}_6\widetilde{\mathcal{B}}_8 - \widetilde{\mathcal{B}}_7^2 + 2\widetilde{\mathcal{B}}_4$, $\sigma_{13} = -2\widetilde{\mathcal{B}}_0\widetilde{\mathcal{B}}_6 + 2\widetilde{\mathcal{B}}_1\widetilde{\mathcal{B}}_5 - 2\widetilde{\mathcal{B}}_2\widetilde{\mathcal{B}}_4 + \widetilde{\mathcal{B}}_3^2 + 2\widetilde{\mathcal{B}}_7\widetilde{\mathcal{B}}_9 - \widetilde{\mathcal{B}}_8^2$, $\sigma_{14} = 2\widetilde{\mathcal{B}}_0\widetilde{\mathcal{B}}_8 - 2\widetilde{\mathcal{B}}_3\widetilde{\mathcal{B}}_5 + \widetilde{\mathcal{B}}_4^2 - \widetilde{\mathcal{B}}_9^2$, $\sigma_{15} = \widetilde{\mathcal{B}}_5^2 - \widetilde{\mathcal{B}}_0^2$. Letting $\theta_1^2 = m_1$ in (B.2), we get

$$m_1^5 + \sigma_{11}m_1^4 + \sigma_{12}m_1^3 + \sigma_{13}m_1^2 + \sigma_{14}m_1 + \sigma_{15} = 0. \tag{B.3}$$

Assume that the above equation has n ($1 \le n \le 5$) positive roots, given by $m_{11}, m_{12}, \ldots m_{1n}$. Then, (B.2) has ($1 \le n \le 5$) positive roots $\theta_{1i} = \sqrt{m_{1i}}$ ($1 \le i \le n$). For θ_{1i}, $\tau_{1i}^{(r)} = \frac{1}{\theta_{1i}}\arccos\left[\frac{N_{11}(\theta_1)N_{13}(\theta_1)+N_{12}(\theta_1)N_{14}(\theta_1)}{N_{11}^2(\theta_1)+N_{12}^2(\theta_1)} + 2r\pi\right], i = 1\ldots n;\quad r = 0, 1, 2\ldots.$ Let us denote $\tau_{10} = \min\left\{\tau_{1i}^{(0)}\right\}$, $i = 1, 2, \ldots n$. From Eq. (B.1), we have $\left[\frac{d\lambda}{d\tau_1}\right]^{-1} = \frac{5\lambda^4+4\widetilde{\mathcal{B}}_1\lambda^3+3\widetilde{\mathcal{B}}_2\lambda^2+2\widetilde{\mathcal{B}}_3\lambda+\widetilde{\mathcal{B}}_4+e^{-\lambda\tau_1}\left(4\widetilde{\mathcal{B}}_6\lambda^3+3\widetilde{\mathcal{B}}_7\lambda^2+2\widetilde{\mathcal{B}}_8\lambda+\widetilde{\mathcal{B}}_9\right)}{e^{-\lambda\tau_1}(\widetilde{\mathcal{B}}_6\lambda^5+\widetilde{\mathcal{B}}_7\lambda^4+\widetilde{\mathcal{B}}_8\lambda^3+\widetilde{\mathcal{B}}_9\lambda^2+\widetilde{\mathcal{B}}_0\lambda)} - \frac{\tau_1}{\lambda}$. Upon substituting $\lambda = i\theta_{10}$, we get, $Re\left[\frac{d\lambda}{d\tau_1}\right]^{-1}_{\tau_1=\tau_{10}} = \frac{Y_{11}Y_{13}+Y_{12}Y_{14}}{Y_{11}^2+Y_{12}^2}$ with $Y_{11} = \theta_{10}^4\widetilde{\mathcal{B}}_6 - \theta_{10}^2\widetilde{\mathcal{B}}_8 + \widetilde{\mathcal{B}}_0$, $Y_{12} = \theta_{10}\widetilde{\mathcal{B}}_9 - \theta_{10}^3\widetilde{\mathcal{B}}_7$, $Y_{13} = \cos\tau_{10}\theta_{10}(2\widetilde{\mathcal{B}}_3 - 4\widetilde{\mathcal{B}}_1\theta_{10}^2) - \sin\tau_{10}\theta_{10}(-5\theta_{10}^3 + 3\widetilde{\mathcal{B}}_2\theta_{10} - \widetilde{\mathcal{B}}_4/\theta_{10}) + 2\widetilde{\mathcal{B}}_8 - 4\theta_{10}^2\widetilde{\mathcal{B}}_6$, $Y_{14} = \sin\tau_{10}\theta_{10}(2\widetilde{\mathcal{B}}_3 - 4\widetilde{\mathcal{B}}_1\theta_{10}^2) + \cos\tau_{10}\theta_{10}(3\widetilde{\mathcal{B}}_2\theta_{10} - 5\theta_{10}^3 - \widetilde{\mathcal{B}}_4/\theta_{10}) + \widetilde{\mathcal{B}}_9 - 3\widetilde{\mathcal{B}}_7\theta_{10}$. Thus, if $Y_{11}Y_{13}+Y_{12}Y_{14}\neq 0$, then $Re[d\lambda/d\tau]^{-1}_{\tau_1=\tau_{10}} \neq 0$. Hence, based on Hopf bifurcation theorem in [28], we have proof of Theorem 3(a).

Proof of Theorem 3(b) $\tau_2 > 0$, $\tau_1 = 0$, and $\tau_3 = 0$: In this case Eq. (8) becomes

$$\lambda^5 + \widetilde{\mathcal{E}}_1\lambda^4 + \widetilde{\mathcal{E}}_2\lambda^3 + \widetilde{\mathcal{E}}_3\lambda^2 + \widetilde{\mathcal{E}}_4\lambda + \widetilde{\mathcal{E}}_5 + e^{-\lambda\tau_1}(\widetilde{\mathcal{E}}_6\lambda^4 + \widetilde{\mathcal{E}}_7\lambda^3 + \widetilde{\mathcal{E}}_8\lambda^2 + \widetilde{\mathcal{E}}_9\lambda + \widetilde{\mathcal{E}}_0) = 0, \tag{B.4}$$

where $\widetilde{\mathcal{E}}_1 = A_{11} + B_{11} + F_{11}$, $\widetilde{\mathcal{E}}_2 = A_{12} + B_{12} + F_{12} + H_{11}$, $\widetilde{\mathcal{E}}_3 = A_{13} + B_{13} + F_{13} + H_{12}$, $\widetilde{\mathcal{E}}_4 = A_{14} + B_{14} + F_{14} + H_{13}$, $\widetilde{\mathcal{E}}_5 = A_{15} + B_{15} + F_{15} + H_{14}$, $\widetilde{\mathcal{E}}_6 = E_{11}$, $\widetilde{\mathcal{E}}_7 = E_{12} + G_{11} + K_{11}$, $\widetilde{\mathcal{E}}_8 = E_{13} + G_{12} + K_{12} + L_{11}$, $\widetilde{\mathcal{E}}_9 = E_{14} + G_{13} + K_{13} + L_{12}$, $\widetilde{\mathcal{E}}_0 = E_{15} + G_{14} + K_{14} + L_{13}$. Let $\lambda = i\theta_2$ ($\theta_2 > 0$) be root of Eq. (B.4) then, $N_{21}(\theta_2)\cos\tau_2\theta_2 + N_{22}(\theta_2)\sin\tau_2\theta_2 = N_{23}(\theta_2)$, and $N_{22}(\theta_2)\cos\tau_2\theta_2 - N_{21}(\theta_2)\sin\tau_2\theta_2 = N_{24}(\theta_2)$ where, $N_{21}(\theta_2) = \widetilde{\mathcal{E}}_6\theta_2^4 - \widetilde{\mathcal{E}}_8\theta_2^2 + \widetilde{\mathcal{E}}_0$, $N_{22}(\theta_2) = \widetilde{\mathcal{E}}_9\theta_2 - \widetilde{\mathcal{E}}_7\theta_2^3$, $N_{23}(\theta_2) = \widetilde{\mathcal{E}}_3\theta_2^2 - \widetilde{\mathcal{E}}_5 - \widetilde{\mathcal{E}}_1\theta_2^4$, $N_{24}(\theta_2) = \widetilde{\mathcal{E}}_2\theta_2^3 - \widetilde{\mathcal{E}}_4\theta_2 - \theta_2^5$. This implies the following equation

$$\theta_2^{10} + \sigma_{21}\theta_2^8 + \sigma_{22}\theta_2^6 + \sigma_{23}\theta_2^4 + \sigma_{24}\theta_2^2 + \sigma_{25} = 0, \tag{B.5}$$

where $\sigma_{21} = \widetilde{\mathcal{E}}_1^2 - \widetilde{\mathcal{E}}_6^2 - 2\widetilde{\mathcal{E}}_2$, $\sigma_{22} = -2\widetilde{\mathcal{E}}_1\widetilde{\mathcal{E}}_3 + \widetilde{\mathcal{E}}_2^2 + 2\widetilde{\mathcal{E}}_6\widetilde{\mathcal{E}}_8 - \widetilde{\mathcal{E}}_7^2 + 2\widetilde{\mathcal{E}}_4$, $\sigma_{23} = -2\widetilde{\mathcal{E}}_0\widetilde{\mathcal{E}}_6 + 2\widetilde{\mathcal{E}}_1\widetilde{\mathcal{E}}_5 - 2\widetilde{\mathcal{E}}_2\widetilde{\mathcal{E}}_4 + \widetilde{\mathcal{E}}_3^2 + 2\widetilde{\mathcal{E}}_7\widetilde{\mathcal{E}}_9 - \widetilde{\mathcal{E}}_8^2$, $\sigma_{24} = 2\widetilde{\mathcal{E}}_0\widetilde{\mathcal{E}}_8 - 2\widetilde{\mathcal{E}}_3\widetilde{\mathcal{E}}_5 + \widetilde{\mathcal{E}}_4^2 - \widetilde{\mathcal{E}}_9^2$, $\sigma_{25} = \widetilde{\mathcal{E}}_5^2 - \widetilde{\mathcal{E}}_0^2$. Let $\theta_2^2 = m_2$, then we get $m_2^5 + \sigma_{21}m_2^4 + \sigma_{22}m_2^3 + \sigma_{23}m_2^2 + \sigma_{24}m_2 + \sigma_{25} = 0$. Assume that the Eq. (5) has n ($1 \le n \le 5$) positive roots, denoted by $m_{21}, m_{22}, \ldots m_{2n}$. Then, (B.5) has ($1 \le n \le 5$) positive roots $\theta_{2i} = \sqrt{m_{2i}}$ ($1 \le i \le n$). For θ_{2i}, $\tau_{2i}^{(r)} = \frac{1}{\theta_{2i}}\arccos\left[\frac{N_{21}(\theta_2)N_{23}(\theta_2)+N_{22}(\theta_2)N_{24}(\theta_2)}{N_{21}^2(\theta_2)+N_{22}^2(\theta_2)} + 2r\pi\right]$. $i = 1\ldots n;\quad r = 0, 1, 2\ldots.$ Let $\tau_{20} = \min\left\{\tau_{2i}^{(0)}\right\}$, $i = 1, 2, \ldots n$ For Eq. (B.4), we have the corresponding roots as $\pm i\theta_{20}$ when $\tau_2 = \tau_{20}$. From (B.4), we obtain $\left[\frac{d\lambda}{d\tau_2}\right]^{-1} = \frac{5\lambda^4+4\widetilde{\mathcal{E}}_1\lambda^3+3\widetilde{\mathcal{E}}_2\lambda^2+2\widetilde{\mathcal{E}}_3\lambda+\widetilde{\mathcal{E}}_4+e^{-\lambda\tau_1}\left(4\widetilde{\mathcal{E}}_6\lambda^3+3\widetilde{\mathcal{E}}_7\lambda^2+2\widetilde{\mathcal{E}}_8\lambda+\widetilde{\mathcal{E}}_9\right)}{e^{-\lambda\tau_2}(\widetilde{\mathcal{E}}_6\lambda^5+\widetilde{\mathcal{E}}_7\lambda^4+\widetilde{\mathcal{E}}_8\lambda^3+\widetilde{\mathcal{E}}_9\lambda^2+\widetilde{\mathcal{E}}_0\lambda)} - \frac{\tau_2}{\lambda}$. Then, $Re\left[\frac{d\lambda}{d\tau_2}\right]^{-1}_{\tau_2=\tau_{20}} = \frac{Y_{21}Y_{23}+Y_{22}Y_{24}}{Y_{21}^2+Y_{22}^2}$ with $Y_{21} = \theta_{20}^4\widetilde{\mathcal{E}}_6 - \theta_{20}^2\widetilde{\mathcal{E}}_8 + \widetilde{\mathcal{E}}_0$, $Y_{22} = \theta_{20}\widetilde{\mathcal{E}}_9 - \theta_{20}^3\widetilde{\mathcal{E}}_7$, $Y_{23} = \cos\tau_{20}\theta_{20}(2\widetilde{\mathcal{E}}_3 - 4\widetilde{\mathcal{E}}_1\theta_{20}^2) - \sin\tau_{20}\theta_{20}(-5\theta_{20}^3 + 3\widetilde{\mathcal{E}}_2\theta_{20} - \widetilde{\mathcal{E}}_4/\theta_{20}) + 2\widetilde{\mathcal{E}}_8 - 4\theta_{20}^2\widetilde{\mathcal{E}}_6$, $Y_{24} = \sin\tau_{20}\theta_{20}(2\widetilde{\mathcal{E}}_3 - 4\widetilde{\mathcal{E}}_1\theta_{20}^2) + \cos\tau_{20}\theta_{20}(3\widetilde{\mathcal{E}}_2\theta_{20} - 5\theta_{20}^3 - \widetilde{\mathcal{E}}_4/\theta_{20}) + \widetilde{\mathcal{E}}_9 - 3\widetilde{\mathcal{E}}_7\theta_{20}$. Thus, if $Y_{21}Y_{23}+Y_{22}Y_{24}\neq 0$, then $Re[d\lambda/d\tau]^{-1}_{\tau_2=\tau_{20}} \neq 0$. Hence, we have the Theorem 3(b).

Proof of Theorem 3(c) $\tau_3 > 0$, $\tau_1 = 0$, and $\tau_2 = 0$.
For $\tau_3 > 0$, $\tau_1 = 0$ and $\tau_2 = 0$, Eq. (8) is modified as follows

$$\lambda^5 + \widetilde{\mathcal{F}}_1\lambda^4 + \widetilde{\mathcal{F}}_2\lambda^3 + \widetilde{\mathcal{F}}_3\lambda^2 + \widetilde{\mathcal{F}}_4\lambda + \widetilde{\mathcal{F}}_5 + e^{-\lambda\tau_3}(\widetilde{\mathcal{F}}_6\lambda^4 + \widetilde{\mathcal{F}}_7\lambda^3 + \widetilde{\mathcal{F}}_8\lambda^2 + \widetilde{\mathcal{F}}_9\lambda + \widetilde{\mathcal{F}}_0) = 0,$$

where $\widetilde{\mathcal{F}}_1 = A_{11} + B_{11} + E_{11}$, $\widetilde{\mathcal{F}}_2 = A_{12} + B_{12} + E_{12} + G_{11}$, $\widetilde{\mathcal{F}}_3 = A_{13} + B_{13} + E_{13} + G_{12}$, $\widetilde{\mathcal{F}}_4 = A_{14} + B_{14} + E_{14} + G_{13}$, $\widetilde{\mathcal{F}}_5 = A_{15} + B_{15} + E_{15} + G_{14}$, $\widetilde{\mathcal{F}}_6 = F_{11}$, $\widetilde{\mathcal{F}}_7 = F_{12} + H_{11} + K_{11}$, $\widetilde{\mathcal{F}}_8 = F_{13} + H_{12} + K_{12} + L_{11}$, $\widetilde{\mathcal{F}}_9 = F_{14} + H_{13} + K_{13} + L_{12}$, $\widetilde{\mathcal{F}}_0 = F_{15} + H_{14} + K_{14} + L_{13}$. Proceeding in the same manner as the above cases, we get $\tau_{3i}^{(r)} = \frac{1}{\theta_{3i}} \arccos\left[\frac{N_{31}(\theta_3)N_{33}(\theta_3)+N_{32}(\theta_3)N_{34}(\theta_3)}{N_{31}^2(\theta_3)+N_{32}^2(\theta_3)} + 2r\pi\right]$. $i = 1\ldots5$; $r = 0, 1, 2\ldots.$ where, $N_{31}(\theta_3) = \widetilde{\mathcal{F}}_6\theta_3^4 - \widetilde{\mathcal{F}}_8\theta_3^2 + \widetilde{\mathcal{F}}_0$, $N_{32}(\theta_3) = \widetilde{\mathcal{F}}_9\theta_3 - \widetilde{\mathcal{F}}_7\theta_3^3$, $N_{33}(\theta_3) = \widetilde{\mathcal{F}}_3\theta_3^2 - \widetilde{\mathcal{F}}_5 - \widetilde{\mathcal{F}}_1\theta_3^4$, $N_{34}(\theta_3) = \widetilde{\mathcal{F}}_2\theta_3^3 - \widetilde{\mathcal{F}}_4\theta_3 - \theta_3^5$. and $\theta_{3i} = \sqrt{m_{3i}}$, $(1 \le i \le 5)$ in which m_{3i}, $i = 1,\ldots5$ are the positive roots of equation $m_3^5 + \sigma_{31}m_3^4 + \sigma_{32}m_3^3 + \sigma_{33}m_3^2 + \sigma_{34}m_3 + \sigma_{35} = 0$ with $\sigma_{31} = \widetilde{\mathcal{F}}_1^2 - \widetilde{\mathcal{F}}_6^2 - 2\widetilde{\mathcal{F}}_2$, $\sigma_{32} = -2\widetilde{\mathcal{F}}_1\widetilde{\mathcal{F}}_3 + \widetilde{\mathcal{F}}_2^2 + 2\widetilde{\mathcal{F}}_6\widetilde{\mathcal{F}}_8 - \widetilde{\mathcal{F}}_7^2 + 2\widetilde{\mathcal{F}}_4$, $\sigma_{33} = -2\widetilde{\mathcal{F}}_0\widetilde{\mathcal{F}}_6 + 2\widetilde{\mathcal{F}}_1\widetilde{\mathcal{F}}_5 - 2\widetilde{\mathcal{F}}_2\widetilde{\mathcal{F}}_4 + \widetilde{\mathcal{F}}_3^2 + 2\widetilde{\mathcal{F}}_7\widetilde{\mathcal{F}}_9 - \widetilde{\mathcal{F}}_8^2$, $\sigma_{34} = 2\widetilde{\mathcal{F}}_0\widetilde{\mathcal{F}}_8 - 2\widetilde{\mathcal{F}}_3\widetilde{\mathcal{F}}_5 + \widetilde{\mathcal{F}}_4^2 - \widetilde{\mathcal{F}}_9^2$, $\sigma_{35} = \widetilde{\mathcal{F}}_5^2 - \widetilde{\mathcal{F}}_0^2$. Thus, we have Theorem 3(c).

Proof of Theorem 3(d) $\tau_1 > 0$, $\tau_2 \in (0, \tau_{20})$, and $\tau_3 \in (0, \tau_{30})$
Letting $\lambda = i\theta_1^*$ in Eq. (8) and equating the real and imaginary parts, we get the following

$$N_{41}(\theta_1^*)\cos\tau_1\theta_1^* + N_{42}(\theta_1^*)\sin\tau_1\theta_1^* = N_{43}(\theta_1^*), \quad \text{and} \quad N_{42}(\theta_1^*)\cos\tau_1\theta_1^* - N_{41}(\theta_1^*)\sin\tau_1\theta_1^* = N_{44}(\theta_1^*),$$

with

$$\begin{aligned}
N_{41}(\theta_1^*) &= (L_{13} - L_{11}\theta_1^{*2})\cos(\tau_2+\tau_3)\theta_1^* + L_{12}\theta_1^*\sin(\tau_2+\tau_3)\theta_1^* + (G_{14} - G_{12}\theta_1^{*2})\cos\tau_2\theta_1^* \\
&\quad + (G_{13}\theta_1^* - G_{11}\theta_1^{*3})\sin\tau_2\theta_1^* + (H_{14} - H_{12}\theta_1^{*2})\cos\tau_3\theta_1^* + (H_{13}\theta_1^* - H_{11}\theta_1^{*3})\sin\tau_3\theta_1^* + B_{15} \\
&\quad - B_{13}\theta_1^{*2} + B_{11}\theta_1^{*4}, \\
N_{42}(\theta_1^*) &= (L_{11}\theta_1^{*2} - L_{13})\sin(\tau_2+\tau_3)\theta_1^* + L_{12}\theta_1^*\cos(\tau_2+\tau_3)\theta_1^* + (G_{12}\theta_1^{*2} - G_{14})\sin\tau_2\theta_1^* \\
&\quad + (G_{13}\theta_1^* - G_{11}\theta_1^{*3})\cos\tau_2\theta_1^* + (H_{12}\theta_1^{*2} - H_{14})\sin\tau_3\theta_1^* + (H_{13}\theta_1^* - H_{11}\theta_1^{*3})\cos\tau_3\theta_1^* \\
&\quad + B_{14}\theta_1^* - B_{12}\theta_1^{*3}, \\
N_{43}(\theta_1^*) &= A_{13}\theta_1^{*2} - A_{11}\theta_1^{*4} - A_{15} + (K_{12}\theta_1^{*2} - K_{14})\cos(\tau_2+\tau_3)\theta_1^* + (K_{11}\theta_1^{*3} - K_{13}\theta_1^*)\sin(\tau_2+\tau_3)\theta_1^* \\
&\quad + (E_{13}\theta_1^{*2} - E_{15} - E_{11}\theta_1^{*4})\cos\tau_2\theta_1^* + (E_{12}\theta_1^{*3} - E_{14}\theta_1^*)\sin\tau_2\theta_1^* + (F_{13}\theta_1^{*2} - F_{15} - F_{11}\theta_1^{*4})\cos\tau_3\theta_1^* \\
&\quad + (F_{12}\theta_1^{*3} - F_{14}\theta_1^*)\sin\tau_3\theta_1^*, \\
N_{44}(\theta_1^*) &= A_{12}\theta_1^{*3} - A_{14}\theta_1^* + (K_{14} - K_{12}\theta_1^{*2})\sin(\tau_2+\tau_3)\theta_1^* + (K_{11}\theta_1^{*3} - K_{13}\theta_1^*)\cos(\tau_2+\tau_3)\theta_1^* \\
&\quad + (E_{11}\theta_1^{*4} - E_{13}\theta_1^{*2} + E_{15})\sin\tau_2\theta_1^* + (E_{12}\theta_1^{*3} - E_{14}\theta_1^*)\cos\tau_2\theta_1^* + (F_{11}\theta_1^{*4} - F_{13}\theta_1^{*2} + F_{15})\sin\tau_3\theta_1^* \\
&\quad + (F_{12}\theta_1^{*3} - F_{14}\theta_1^*)\cos\tau_3\theta_1^*.
\end{aligned}$$

It can be seen that, $N_{43}^2(\theta_1^*) + N_{44}^2(\theta_1^*) = N_{41}^2(\theta_1^*) + N_{42}^2(\theta_1^*)$. Let us assume that $\theta_{11}^*, \theta_{12}^*, \ldots \theta_{1n}^*$ are the finite positive roots of the above equation. Then for θ_{1i}^*, we have $\tau_{1i}^* = \frac{1}{\theta_{1i}^*}\arccos\left[\frac{N_{41}(\theta_1^*)N_{43}(\theta_1^*)+N_{42}(\theta_1^*)N_{44}(\theta_1^*)}{N_{41}^2(\theta_1^*)+N_{42}^2(\theta_1^*)} + 2r\pi\right]$. $i = 1\ldots n$; $r = 0, 1, 2\ldots.$ Let $\tau_1^* = \min\left\{\tau_{1i}^{(0)}\right\}$, $i = 1, 2, \ldots n$.
Hence, for $\tau_1 = \tau_1^*$, from Eq. (8), we have $\left[\frac{d\lambda}{d\tau_1}\right]^{-1} = \frac{\Gamma_1(\lambda)}{\Gamma_2(\lambda)}$ where

$$\begin{aligned}
\Gamma_1(\lambda) &= 5\lambda^4 + 4A_{11}\lambda^3 + 3A_{12}\lambda^2 + 2A_{13}\lambda + A_{14} - \tau_1 e^{-\lambda\tau_1}\left(\lambda^4 B_{11} + \lambda^3 B_{12} + \lambda^2 B_{13} + \lambda B_{14} + B_{15}\right) \\
&\quad + e^{-\lambda\tau_1}\left(4\lambda^3 B_{11} + 3\lambda^2 B_{12} + 2\lambda B_{13} + B_{14}\right) - \tau_2 e^{-\lambda\tau_2}\left(\lambda^4 E_{11} + \lambda^3 E_{12} + \lambda^2 E_{13} + \lambda E_{14} + E_{15}\right) \\
&\quad + e^{-\lambda\tau_2}\left(4\lambda^3 E_{11} + 3\lambda^2 E_{12} + 2\lambda E_{13} + E_{14}\right) - \tau_3 e^{-\lambda\tau_3}\left(\lambda^4 F_{11} + \lambda^3 F_{12} + \lambda^2 F_{13} + \lambda F_{14} + F_{15}\right) \\
&\quad + e^{-\lambda\tau_3}\left(4\lambda^3 F_{11} + 3\lambda^2 F_{12} + 2\lambda F_{13} + F_{14}\right) + (-\tau_1 - \tau_2)e^{-\lambda(\tau_1+\tau_2)}\left(\lambda^3 G_{11} + \lambda^2 G_{12} + \lambda G_{13} + G_{14}\right) \\
&\quad + e^{-\lambda(\tau_1+\tau_2)}\left(3\lambda^2 G_{11} + 2\lambda G_{12} + G_{13}\right) + (-\tau_1 - \tau_3)e^{-\lambda(\tau_1+\tau_3)}\left(\lambda^3 H_{11} + \lambda^2 H_{12} + \lambda H_{13} + H_{14}\right) \\
&\quad + e^{-\lambda(\tau_1+\tau_3)}\left(3\lambda^2 H_{11} + 2\lambda H_{12} + H_{13}\right) + (-\tau_2 - \tau_3)e^{-\lambda(\tau_2+\tau_3)}\left(\lambda^3 K_{11} + \lambda^2 K_{12} + \lambda K_{13} + K_{14}\right) \\
&\quad + e^{-\lambda(\tau_2+\tau_3)}\left(3\lambda^2 K_{11} + 2\lambda K_{12} + K_{13}\right) + (-\tau_1 - \tau_2 - \tau_3)e^{-\lambda(\tau_1+\tau_2+\tau_3)}\left(\lambda^2 L_{11} + \lambda L_{12} + L_{13}\right) \\
&\quad + e^{-\lambda(\tau_1+\tau_2+\tau_3)}\left(2\lambda L_{11} + L_{12}\right), \\
\Gamma_2(\lambda) &= \lambda e^{-\lambda\tau_1}\left(\lambda^4 B_{11} + \lambda^3 B_{12} + \lambda^2 B_{13} + \lambda B_{14} + B_{15}\right) + \lambda e^{-\lambda(\tau_1+\tau_2)}\left(\lambda^3 G_{11} + \lambda^2 G_{12} + \lambda G_{13} + G_{14}\right) \\
&\quad + \lambda e^{-\lambda(\tau_1+\tau_3)}\left(\lambda^3 H_{11} + \lambda^2 H_{12} + \lambda H_{13} + H_{14}\right) + \lambda e^{-\lambda(\tau_1+\tau_2+\tau_3)}\left(\lambda^2 L_{11} + \lambda L_{12} + L_{13}\right).
\end{aligned}$$

Then, we get $Re\left[\frac{d\lambda}{d\tau_1}\right]^{-1}_{\tau_1=\tau_1^*} = \frac{Y_{41}Y_{43}+Y_{42}Y_{44}}{Y_{41}^2+Y_{42}^2}$. Here,

$$
\begin{aligned}
Y_{41} &= \theta_1^* \sin(\theta_1^*\tau_1^*)\left(\theta_1^{*4}B_{11} - \theta_1^{*2}B_{13} + B_{15}\right) - \theta_1^* \cos(\theta_1^*\tau_1^*)\left(B_{14}\theta_1^* - B_{12}\theta_1^{*3}\right) + \theta_1^* \sin(\theta_1^*\tau_1^* + \theta_1^*\tau_2)\left(G_{14} - \theta_1^{*2}G_{12}\right)\\
&\quad - \theta_1^* \cos(\theta_1^*\tau_1^* + \theta_1^*\tau_2)\left(-G_{11}\theta_1^{*3} + G_{13}\theta_1^*\right) + \theta_1^* \sin(\theta_1^*\tau_1^* + \theta_1^*\tau_3)\left(-\theta_1^{*2}H_{12} + H_{14}\right)\\
&\quad - \theta_1^* \cos(\theta_1^*\tau_1^* + \theta_1^*\tau_3)\left(-H_{11}\theta_1^{*3} + H_{13}\theta_1^*\right) + \theta_1^* \sin(\theta_1^*\tau_1^* + \theta_1^*\tau_2 + \theta_1^*\tau_3)\left(-\theta_1^{*2}L_{11} + L_{13}\right)\\
&\quad - \theta_1^{*2} \cos(\theta_1^*\tau_1^* + \theta_1^*\tau_2 + \theta_1^*\tau_3)\, L_{12},\\
Y_{42} &= \theta_1^* \cos(\theta_1^*\tau_1^*)\left(\theta_1^{*4}B_{11} - \theta_1^{*2}B_{13} + B_{15}\right) + \theta_1^* \sin(\theta_1^*\tau_1^*)\left(-B_{12}\theta_1^{*3} + B_{14}\theta_1^*\right) + \theta_1^* \cos(\theta_1^*\tau_1^* + \theta_1^*\tau_2)\left(-\theta_1^{*2}G_{12} + G_{14}\right)\\
&\quad + \theta_1^* \sin(\theta_1^*\tau_1^* + \theta_1^*\tau_2)\left(-G_{11}\theta_1^{*3} + G_{13}\theta_1^*\right) + \theta_1^* \cos(\theta_1^*\tau_1^* + \theta_1^*\tau_3)\left(-\theta_1^{*2}H_{12} + H_{14}\right) + \theta_1^* \sin(\theta_1^*\tau_1^* + \theta_1^*\tau_3)\left(-H_{11}\theta_1^{*3}\right)\\
&\quad + \theta_1^* \cos(\theta_1^*\tau_1^* + \theta_1^*\tau_2 + \theta_1^*\tau_3)\left(-\theta_1^{*2}L_{11} + L_{13}\right) + \theta_1^{*2} \sin(\theta_1^*\tau_1^* + \theta_1^*\tau_2 + \theta_1^*\tau_3)\, L_{12},\\
Y_{43} &= \left(L_{11}(\tau_1^* + \tau_2 + \tau_3)\theta_1^{*2} - L_{13}\tau_1^* - L_{13}\tau_2 - L_{13}\tau_3 + L_{12}\right)\cos(\theta_1^*(\tau_1^* + \tau_2 + \tau_3))\\
&\quad + 2\theta_1^*(-1/2\, L_{12}\tau_1^* - 1/2\, L_{12}\tau_2 - 1/2\, L_{12}\tau_3 + L_{11})\sin(\theta_1^*(\tau_1^* + \tau_2 + \tau_3))\\
&\quad + \left((G_{12}\tau_1^* + G_{12}\tau_2 - 3\, G_{11})\theta_1^{*2} - G_{14}\tau_1^* - G_{14}\tau_2 + G_{13}\right)\cos(\theta_1^*(\tau_1^* + \tau_2))\\
&\quad + \left((H_{12}\tau_1^* + H_{12}\tau_3 - 3\, H_{11})\theta_1^{*2} - H_{14}\tau_1^* - H_{14}\tau_3 + H_{13}\right)\cos(\theta_1^*(\tau_1^* + \tau_3))\\
&\quad + \left((K_{12}\tau_2 + K_{12}\tau_3 - 3\, K_{11})\theta_1^{*2} - K_{14}\tau_2 - K_{14}\tau_3 + K_{13}\right)\cos(\theta_1^*(\tau_2 + \tau_3))\\
&\quad + \left(G_{11}(\tau_1^* + \tau_2)\theta_1^{*2} - G_{13}\tau_1^* - G_{13}\tau_2 + 2\, G_{12}\right)\theta_1^*\sin(\theta_1^*(\tau_1^* + \tau_2))\\
&\quad + \theta_1^*\left(H_{11}(\tau_1^* + \tau_3)\theta_1^{*2} - H_{13}\tau_1^* - H_{13}\tau_3 + 2\, H_{12}\right)\sin(\theta_1^*(\tau_1^* + \tau_3))\\
&\quad + \theta_1^*\left(K_{11}(\tau_2 + \tau_3)\theta_1^{*2} - K_{13}\tau_2 - K_{13}\tau_3 + 2\, K_{12}\right)\sin(\theta_1^*(\tau_2 + \tau_3))\\
&\quad + \left(-B_{11}\tau_1^*\theta_1^{*4} + (B_{13}\tau_1^* - 3\, B_{12})\theta_1^{*2} - B_{15}\tau_1^* + B_{14}\right)\cos(\theta_1^*\tau_1^*)\\
&\quad + \left(-E_{11}\tau_2\theta_1^{*4} + (E_{13}\tau_2 - 3\, E_{12})\theta_1^{*2} - E_{15}\tau_2 + E_{14}\right)\cos(\theta_1^*\tau_2)\\
&\quad + \left(-F_{11}\tau_3\theta_1^{*4} + (F_{13}\tau_3 - 3\, F_{12})\theta_1^{*2} - F_{15}\tau_3 + F_{14}\right)\cos(\theta_1^*\tau_3)\\
&\quad - 4\theta_1^*\left((-1/4\,\tau_1^* B_{12} + B_{11})\theta_1^{*2} + 1/4\,\tau_1^* B_{14} - 1/2\, B_{13}\right)\sin(\theta_1^*\tau_1^*)\\
&\quad + 2\theta_1^*\left((1/2\,\tau_2 E_{12} - 2\, E_{11})\theta_1^{*2} - 1/2\, E_{14}\tau_2 + E_{13}\right)\sin(\theta_1^*\tau_2)\\
&\quad - 4\theta_1^*\left((-1/4\, F_{12}\tau_3 + F_{11})\theta_1^{*2} + 1/4\, F_{14}\tau_3 - 1/2\, F_{13}\right)\sin(\theta_1^*\tau_3) + 5\theta_1^{*4} - 3\, A_{12}\theta_1^{*2} + A_{14},\\
Y_{44} &= \left(-L_{11}(\tau_1^* + \tau_2 + \tau_3)\theta_1^{*2} + L_{13}\tau_1^* + L_{13}\tau_2 + L_{13}\tau_3 - L_{12}\right)\sin(\theta_1^*(\tau_1^* + \tau_2 + \tau_3))\\
&\quad + 2\,(-1/2\, L_{12}\tau_1^* - 1/2\, L_{12}\tau_2 - 1/2\, L_{12}\tau_3 + L_{11})\theta_1^*\cos(\theta_1^*(\tau_1^* + \tau_2 + \tau_3))\\
&\quad + \left((-G_{12}\tau_1^* - G_{12}\tau_2 + 3\, G_{11})\theta_1^{*2} + G_{14}\tau_1^* + G_{14}\tau_2 - G_{13}\right)\sin(\theta_1^*(\tau_1^* + \tau_2))\\
&\quad + \left((-H_{12}\tau_1^* - H_{12}\tau_3 + 3\, H_{11})\theta_1^{*2} + H_{14}\tau_1^* + H_{14}\tau_3 - H_{13}\right)\sin(\theta_1^*(\tau_1^* + \tau_3))\\
&\quad + \left((-K_{12}\tau_2 - K_{12}\tau_3 + 3\, K_{11})\theta_1^{*2} + K_{14}\tau_2 + K_{14}\tau_3 - K_{13}\right)\sin(\theta_1^*(\tau_2 + \tau_3))\\
&\quad + \theta_1^*\left(G_{11}(\tau_1^* + \tau_2)\theta_1^{*2} - G_{13}\tau_1^* - G_{13}\tau_2 + 2\, G_{12}\right)\cos(\theta_1^*(\tau_1^* + \tau_2))\\
&\quad + \theta_1^*\left(H_{11}(\tau_1^* + \tau_3)\theta_1^{*2} - H_{13}\tau_1^* - H_{13}\tau_3 + 2\, H_{12}\right)\cos(\theta_1^*(\tau_1^* + \tau_3))\\
&\quad + \theta_1^*\left(K_{11}(\tau_2 + \tau_3)\theta_1^{*2} - K_{13}\tau_2 - K_{13}\tau_3 + 2\, K_{12}\right)\cos(\theta_1^*(\tau_2 + \tau_3))\\
&\quad + \left(B_{11}\tau_1^*\theta_1^{*4} + (-B_{13}\tau_1^* + 3\, B_{12})\theta_1^{*2} + B_{15}\tau_1^* - B_{14}\right)\sin(\tau_1^*\theta_1^*)\\
&\quad + \left(E_{11}\tau_2\theta_1^{*4} + (-E_{13}\tau_2 + 3\, E_{12})\theta_1^{*2} + E_{15}\tau_2 - E_{14}\right)\sin(\tau_2\theta_1^*)\\
&\quad + \left(F_{11}\tau_3\theta_1^{*4} + (-F_{13}\tau_3 + 3\, F_{12})\theta_1^{*2} + F_{15}\tau_3 - F_{14}\right)\sin(\tau_3\theta_1^*)\\
&\quad - 4\theta_1^*\left(\left((-1/4\,\tau_1^* B_{12} + B_{11})\theta_1^{*2} + 1/4\,\tau_1^* B_{14} - 1/2\, B_{13}\right)\cos(\tau_1^*\theta_1^*)\right.\\
&\quad + \left((E_{11} - 1/4\,\tau_2 E_{12})\theta_1^{*2} + 1/4\, E_{14}\tau_2 - 1/2\, E_{13}\right)\cos(\tau_2\theta_1^*)
\end{aligned}
$$

$$+\left(\left(-1/4\,F_{12}\tau_3+F_{11}\right)\theta_1^{*2}+1/4\,F_{14}\tau_3-1/2\,F_{13}\right)\cos\left(\tau_3\theta_1^*\right)-1/2\,A_{13}+A_{11}\theta_1^{*2}\,).$$

Thus, if $Y_{41}Y_{43}+Y_{42}Y_{44}\neq 0$, then $Re[d\lambda/d\tau_1]^{-1}_{\tau_1=\tau_1^*}\neq 0$ and thus we have the Theorem 3(d)

Proof of Theorem 3(e) $\tau_1\in(0,\tau_{10})$, $\tau_2>0$, and $\tau_3\in(0,\tau_{30})$
Putting $\lambda=i\theta_2^*$ into Eq. (8), we have $N_{51}(\theta_2^*)\cos\tau_2\theta_2^*+N_{52}(\theta_2^*)\sin\tau_2\theta_2^*=N_{53}(\theta_2^*)$, and $N_{52}(\theta_2^*)\cos\tau_2\theta_2^*-N_{51}(\theta_2^*)\sin\tau_2\theta_2^*=N_{54}(\theta_2^*)$ with

$$\begin{aligned}
N_{51}(\theta_2^*)&=\left(-L_{11}\theta_2^{*2}-L_{13}\right)\cos\left(\theta_2^*\left(\tau_1+\tau_3\right)\right)+L_{12}\theta_2^*\sin\left(\theta_2^*\left(\tau_1+\tau_3\right)\right)+\left(-G_{12}\theta_2^{*2}+G_{14}\right)\cos\left(\theta_2^*\tau_1\right)\\
&+\left(-K_{12}\theta_2^{*2}+K_{14}\right)\cos\left(\theta_2^*\tau_3\right)+\left(-G_{11}\theta_2^{*3}+G_{13}\theta_2^*\right)\sin\left(\theta_2^*\tau_1\right)+\theta_2^*\left(-K_{11}\theta_2^{*2}+K_{13}\right)\sin\left(\theta_2^*\tau_3\right)\\
&+E_{11}\theta_2^{*4}-E_{13}\theta_2^{*2}+E_{15},\\
N_{52}(\theta_2^*)&=\left(L_{11}\theta_2^{*2}-L_{13}\right)\sin\left(\theta_2^*\left(\tau_1+\tau_3\right)\right)-L_{12}\theta_2^*\cos\left(\theta_2^*\left(\tau_1+\tau_3\right)\right)+\left(-G_{11}\theta_2^{*3}+G_{13}\theta_2^*\right)\cos\left(\theta_2^*\tau_1\right)\\
&+\left(-K_{11}\theta_2^{*3}+K_{13}\theta_2^*\right)\cos\left(\theta_2^*\tau_3\right)+\left(G_{12}\theta_2^{*2}-G_{14}\right)\sin\left(\theta_2^*\tau_1\right)+\left(K_{12}\theta_2^{*2}-K_{14}\right)\sin\left(\theta_2^*\tau_3\right)\\
&-E_{12}\theta_2^{*3}+E_{14}\theta_2^*,\\
N_{53}(\theta_2^*)&=\left(H_{12}\theta_2^{*2}-H_{14}\right)\cos\left(\theta_2^*\left(\tau_1+\tau_3\right)\right)+\theta_2^*\left(H_{11}\theta_2^{*2}-H_{13}\right)\sin\left(\theta_2^*\left(\tau_1+\tau_3\right)\right)\\
&+\left(-B_{11}\theta_2^{*4}+B_{13}\theta_2^{*2}-B_{15}\right)\cos\left(\theta_2^*\tau_1\right)+\left(-F_{11}\theta_2^{*4}+F_{13}\theta_2^{*2}-F_{15}\right)\cos\left(\theta_2\tau_3\right)\\
&+\theta_2^*\left(B_{12}\theta_2^{*2}-B_{14}\right)\sin\left(\theta_2^*\tau_1\right)+\theta_2^*\left(F_{12}\theta_2^{*2}-F_{14}\right)\sin\left(\theta_2^*\tau_3\right)-A_{11}\theta_2^{*4}+A_{13}\theta_2^{*2}-A_{15},\\
N_{54}(\theta_2^*)&=\theta_2\left(H_{11}\theta_2-H_{13}\right)\cos\left(\theta_2\left(\tau_1+\tau_3\right)\right)+\left(-H_{12}{\theta_2}^2+H_{14}\right)\sin\left(\theta_2\left(\tau_1+\tau_3\right)\right)\\
&+\sin\left(\theta_2\tau_1\right)\left(B_{11}{\theta_2}^4-B_{13}{\theta_2}^2+B_{15}\right)+\sin\left(\theta_2\tau_3\right)\left(F_{11}{\theta_2}^4-F_{13}{\theta_2}^2+F_{15}\right)\\
&+\theta_2\left(\left(B_{12}{\theta_2}^2-B_{14}\right)\cos\left(\theta_2\tau_1\right)+\left(F_{12}{\theta_2}^2-F_{14}\right)\cos\left(\theta_2\tau_3\right)-{\theta_2}^4+A_{12}{\theta_2}^2-A_{14}\right).
\end{aligned}$$

The characteristic equation with respect to θ_2^* is $N_{53}^2(\theta_2^*)+N_{54}^2(\theta_2^*)-N_{51}^2(\theta_2^*)-N_{52}^2(\theta_2^*)=0$. If $\theta_{21}^*,\theta_{22}^*,\ldots,\theta_{2n}^*$ are the finite positive roots of the above equation. Then for θ_{2i}^*, we have $\tau_{2i}^*=\frac{1}{\theta_{2i}^*}\arccos\left[\frac{N_{51}(\theta_2^*)N_{53}(\theta_2^*)+N_{52}(\theta_2^*)N_{54}(\theta_2^*)}{N_{51}^2(\theta_2^*)+N_{52}^2(\theta_2^*)}+2r\pi\right]$. $i=1\ldots,n;\quad r=0,1,2\ldots$. Let $\tau_2^*=\min\{\tau_{2i}^*\},\quad i=1,2,\ldots,n$. Hence, for $\tau_2=\tau_2^*$, from Eq. (8), we have $Re\left[\frac{d\lambda}{d\tau_2}\right]^{-1}_{\tau_2=\tau_2^*}=\frac{Y_{51}Y_{53}+Y_{52}Y_{54}}{Y_{51}^2+Y_{52}^2}$, where

$$\begin{aligned}
Y_{51}&=\theta_2^*\sin\left(\theta_2^*\tau_2^*\right)\left(E_{11}\theta_2^{*4}-E_{13}\theta_2^{*2}+E_{15}\right)-\theta_2^*\cos\left(\theta_2^*\tau_2^*\right)\left(-E_{12}\theta_2^{*3}+E_{14}\theta_2^*\right)+\theta_2^*\sin\left(\theta_2^*\tau_1+\theta_2^*\tau_2^*\right)\left(-G_{12}\theta_2^{*2}+G_{14}\right)\\
&-\theta_2^*\cos\left(\theta_2^*\tau_1+\theta_2^*\tau_2^*\right)\left(-G_{11}\theta_2^{*3}+G_{13}\theta_2^*\right)+\theta_2^*\sin\left(\theta_2^*\tau_2^*+\theta_2^*\tau_3\right)\left(-K_{12}\theta_2^{*2}+K_{14}\right)\\
&-\theta_2^*\cos\left(\theta_2^*\tau_2^*+\theta_2^*\tau_3\right)\left(-K_{11}\theta_2^{*3}+K_{13}\theta_2^*\right)+\theta_2^*\sin\left(\theta_2^*\tau_1+\theta_2^*\tau_2^*+\theta_2^*\tau_3\right)\left(-L_{11}\theta_2^{*2}+L_{13}\right)\\
&-\theta_2^{*2}\cos\left(\theta_2^*\tau_1+\theta_2^*\tau_2^*+\theta_2^*\tau_3\right)L_{12},\\
Y_{52}&=\theta_2^*\cos\left(\theta_2^*\tau_2^*\right)\left(E_{11}\theta_2^{*4}-E_{13}\theta_2^{*2}+E_{15}\right)+\theta_2^*\sin\left(\theta_2^*\tau_2^*\right)\left(-E_{12}\theta_2^{*3}+E_{14}\theta_2^*\right)+\theta_2^*\cos\left(\theta_2^*\tau_1+\theta_2^*\tau_2^*\right)\left(-G_{12}\theta_2^{*2}+G_{14}\right)\\
&+\theta_2^*\sin\left(\theta_2^*\tau_1+\theta_2^*\tau_2^*\right)\left(-G_{11}\theta_2^{*3}+G_{13}\theta_2^*\right)+\theta_2^*\cos\left(\theta_2^*\tau_2^*+\theta_2^*\tau_3\right)\left(-K_{12}\theta_2^{*2}+K_{14}\right)\\
&+\theta_2^*\sin\left(\theta_2^*\tau_2^*+\theta_2^*\tau_3\right)\left(-K_{11}\theta_2^{*3}+K_{13}\theta_2^*\right)+\theta_2^*\cos\left(\theta_2^*\tau_1+\theta_2^*\tau_2^*+\theta_2^*\tau_3\right)\left(-L_{11}\theta_2^{*2}+L_{13}\right)\\
&+\theta_2^{*2}\sin\left(\theta_2^*\tau_1+\theta_2^*\tau_2^*+\theta_2^*\tau_3\right)L_{12},\\
Y_{53}&=\left(L_{11}\left(\tau_1+\tau_2^*+\tau_3\right)\theta_2^{*2}-L_{13}\tau_1-L_{13}\tau_2^*-L_{13}\tau_3+L_{12}\right)\cos\left(\theta_2^*\left(\tau_1+\tau_2^*+\tau_3\right)\right)\\
&+2\left(-1/2\,L_{12}\tau_1-1/2\,L_{12}\tau_2^*-1/2\,L_{12}\tau_3+L_{11}\right)\theta_2^*\sin\left(\theta_2^*\left(\tau_1+\tau_2^*+\tau_3\right)\right)\\
&+\left(\left(G_{12}\tau_1+G_{12}\tau_2^*-3\,G_{11}\right)\theta_2^{*2}-G_{14}\tau_1-G_{14}\tau_2^*+G_{13}\right)\cos\left(\theta_2^*\left(\tau_1+\tau_2^*\right)\right)\\
&+\left(\left(H_{12}\tau_1+H_{12}\tau_3-3\,H_{11}\right)\theta_2^{*2}-H_{14}\tau_1-H_{14}\tau_3+H_{13}\right)\cos\left(\theta_2^*\left(\tau_1+\tau_3\right)\right)\\
&+\left(\left(K_{12}\tau_2^*+K_{12}\tau_3-3\,K_{11}\right)\theta_2^{*2}-K_{14}\tau_2^*-K_{14}\tau_3+K_{13}\right)\cos\left(\theta_2^*\left(\tau_2^*+\tau_3\right)\right)\\
&+\left(G_{11}\left(\tau_1+\tau_2^*\right)\theta_2^{*2}-G_{13}\tau_1-G_{13}\tau_2^*+2\,G_{12}\right)\theta_2^*\sin\left(\theta_2^*\left(\tau_1+\tau_2^*\right)\right)
\end{aligned}$$

$$
\begin{aligned}
&+\left(H_{11}\left(\tau_1+\tau_3\right)\theta_2^{*2}-H_{13}\tau_1-H_{13}\tau_3+2\,H_{12}\right)\theta_2^{*}\sin\left(\theta_2^{*}\left(\tau_1+\tau_3\right)\right)\\
&+\theta_2^{*}\left(K_{11}\left(\tau_2^{*}+\tau_3\right)\theta_2^{*2}-K_{13}\tau_2^{*}-K_{13}\tau_3+2\,K_{12}\right)\sin\left(\theta_2^{*}\left(\tau_2^{*}+\tau_3\right)\right)\\
&+\left(-B_{11}\tau_1\theta_2^{*4}+\left(B_{13}\tau_1-3\,B_{12}\right)\theta_2^{*2}-B_{15}\tau_1+B_{14}\right)\cos\left(\theta_2^{*}\tau_1\right)\\
&+\left(-E_{11}\tau_2^{*}\theta_2^{*4}+\left(E_{13}\tau_2^{*}-3\,E_{12}\right)\theta_2^{*2}-E_{15}\tau_2^{*}+E_{14}\right)\cos\left(\theta_2^{*}\tau_2^{*}\right)\\
&+\left(-F_{11}\tau_3\theta_2^{*4}+\left(F_{13}\tau_3-3\,F_{12}\right)\theta_2^{*2}-F_{15}\tau_3+F_{14}\right)\cos\left(\theta_2^{*}\tau_3\right)\\
&-4\,\left(\left(-1/4\,\tau_1B_{12}+B_{11}\right)\theta_2^{*2}+1/4\,\tau_1B_{14}-1/2\,B_{13}\right)\theta_2^{*}\sin\left(\theta_2^{*}\tau_1\right)\\
&+2\,\left(\left(1/2\,\tau_2^{*}E_{12}-2\,E_{11}\right)\theta_2^{*2}-1/2\,E_{14}\tau_2^{*}+E_{13}\right)\theta_2^{*}\sin\left(\theta_2^{*}\tau_2^{*}\right)\\
&-4\,\theta_2^{*}\left(\left(-1/4\,F_{12}\tau_3+F_{11}\right)\theta_2^{*2}+1/4\,F_{14}\tau_3-1/2\,F_{13}\right)\sin\left(\theta_2^{*}\tau_3\right)+5\,\theta_2^{*4}-3\,A_{12}\theta_2^{*2}+A_{14},\\
\mathrm{Y}_{54}=&\left(-L_{11}\left(\tau_1+\tau_2^{*}+\tau_3\right)\theta_2^{*2}+L_{13}\tau_1+L_{13}\tau_2^{*}+L_{13}\tau_3-L_{12}\right)\sin\left(\theta_2^{*}\left(\tau_1+\tau_2^{*}+\tau_3\right)\right)\\
&+2\,\theta_2^{*}\left(-1/2\,L_{12}\tau_1-1/2\,L_{12}\tau_2^{*}-1/2\,L_{12}\tau_3+L_{11}\right)\cos\left(\theta_2^{*}\left(\tau_1+\tau_2^{*}+\tau_3\right)\right)\\
&+\left(\left(-G_{12}\tau_1-G_{12}\tau_2^{*}+3\,G_{11}\right)\theta_2^{*2}+G_{14}\tau_1+G_{14}\tau_2^{*}-G_{13}\right)\sin\left(\theta_2^{*}\left(\tau_1+\tau_2^{*}\right)\right)\\
&+\left(\left(-H_{12}\tau_1-H_{12}\tau_3+3\,H_{11}\right)\theta_2^{*2}+H_{14}\tau_1+H_{14}\tau_3-H_{13}\right)\sin\left(\theta_2^{*}\left(\tau_1+\tau_3\right)\right)\\
&+\left(\left(-K_{12}\tau_2^{*}-K_{12}\tau_3+3\,K_{11}\right)\theta_2^{*2}+K_{14}\tau_2^{*}+K_{14}\tau_3-K_{13}\right)\sin\left(\theta_2^{*}\left(\tau_2^{*}+\tau_3\right)\right)\\
&+\theta_2^{*}\left(G_{11}\left(\tau_1+\tau_2^{*}\right)\theta_2^{*2}-G_{13}\tau_1-G_{13}\tau_2^{*}+2\,G_{12}\right)\cos\left(\theta_2^{*}\left(\tau_1+\tau_2^{*}\right)\right)\\
&+\left(H_{11}\left(\tau_1+\tau_3\right)\theta_2^{*2}-H_{13}\tau_1-H_{13}\tau_3+2\,H_{12}\right)\theta_2^{*}\cos\left(\theta_2^{*}\left(\tau_1+\tau_3\right)\right)\\
&+\theta_2^{*}\left(K_{11}\left(\tau_2^{*}+\tau_3\right)\theta_2^{*2}-K_{13}\tau_2^{*}-K_{13}\tau_3+2\,K_{12}\right)\cos\left(\theta_2^{*}\left(\tau_2^{*}+\tau_3\right)\right)\\
&+\left(B_{11}\tau_1\theta_2^{*4}+\left(-B_{13}\tau_1+3\,B_{12}\right)\theta_2^{*2}+B_{15}\tau_1-B_{14}\right)\sin\left(\theta_2^{*}\tau_1\right)\\
&+\left(E_{11}\tau_2^{*}\theta_2^{*4}+\left(-E_{13}\tau_2^{*}+3\,E_{12}\right)\theta_2^{*2}+E_{15}\tau_2^{*}-E_{14}\right)\sin\left(\theta_2^{*}\tau_2^{*}\right)\\
&+\left(F_{11}\tau_3\theta_2^{*4}+\left(-F_{13}\tau_3+3\,F_{12}\right)\theta_2^{*2}+F_{15}\tau_3-F_{14}\right)\sin\left(\theta_2^{*}\tau_3\right)\\
&-4\,\theta_2^{*}\left(\left(\left(-1/4\,\tau_1B_{12}+B_{11}\right)\theta_2^{*2}+1/4\,\tau_1B_{14}-1/2\,B_{13}\right)\cos\left(\theta_2^{*}\tau_1\right)\right.\\
&+\left(\left(E_{11}-1/4\,\tau_2^{*}E_{12}\right)\theta_2^{*2}+1/4\,E_{14}\tau_2^{*}-1/2\,E_{13}\right)\cos\left(\theta_2^{*}\tau_2^{*}\right)\\
&\left.+\left(\left(-1/4\,F_{12}\tau_3+F_{11}\right)\theta_2^{*2}+1/4\,F_{14}\tau_3-1/2\,F_{13}\right)\cos\left(\theta_2^{*}\tau_3\right)-1/2\,A_{13}+A_{11}\theta_2^{*2}\right).
\end{aligned}
$$

Similar to case 4, it can be concluded that if $\mathrm{Y}_{51}\mathrm{Y}_{53}+\mathrm{Y}_{52}\mathrm{Y}_{54}\neq 0$ then, $Re\left[d\lambda/d\tau_2\right]^{-1}_{\tau_2=\tau_2^{*}}\neq 0$. Thus, we have the Theorem 3(e).

Proof of Theorem 3(f) $\tau_1\in(0,\tau_{10})$, $\tau_2\in(0,\tau_{20})$ and $\tau_3>0$: Let us assume $\lambda=i\theta_3^{*}$ be the root of Eq. (8), then we have $N_{61}(\theta_3^{*})\cos\tau_3\theta_3^{*}+N_{62}(\theta_3^{*})\sin\tau_3\theta_3^{*}=N_{63}(\theta_3^{*})$ and $N_{62}(\theta_3^{*})\cos\tau_3\theta_3^{*}-N_{61}(\theta_3^{*})\sin\tau_3\theta_3^{*}=N_{64}(\theta_3^{*})$ where

$$
\begin{aligned}
N_{61}(\theta_3^{*})=&\left(-L_{11}\theta_3^{*2}+L_{13}\right)\cos\left(\theta_3^{*}\left(\tau_1+\tau_2\right)\right)+L_{12}\theta_3^{*}\sin\left(\theta_3^{*}\left(\tau_1+\tau_2\right)\right)+\left(-H_{12}\theta_3^{*2}+H_{14}\right)\cos\left(\theta_3^{*}\tau_1\right)\\
&+\left(-K_{12}\theta_3^{*2}+K_{14}\right)\cos\left(\theta_3^{*}\tau_2\right)+\left(-H_{11}\theta_3^{*3}+H_{13}\theta_3^{*}\right)\sin\left(\theta_3^{*}\tau_1\right)+\theta_3^{*}\left(-K_{11}\theta_3^{*2}+K_{13}\right)\sin\left(\theta_3^{*}\tau_2\right)\\
&+F_{11}\theta_3^{*4}-F_{13}\theta_3^{*2}+F_{15},\\
N_{62}(\theta_3^{*})=&\left(L_{11}\theta_3^{*2}-L_{13}\right)\sin\left(\theta_3^{*}\left(\tau_1+\tau_2\right)\right)+L_{12}\theta_3^{*}\cos\left(\theta_3^{*}\left(\tau_1+\tau_2\right)\right)+\left(-H_{11}\theta_3^{*3}+H_{13}\theta_3^{*}\right)\cos\left(\theta_3^{*}\tau_1\right)\\
&+\left(-K_{11}\theta_3^{*3}+K_{13}\theta_3^{*}\right)\cos\left(\theta_3^{*}\tau_2\right)+\left(H_{12}\theta_3^{*2}-H_{14}\right)\sin\left(\theta_3^{*}\tau_1\right)+\left(K_{12}\theta_3^{*2}-K_{14}\right)\sin\left(\theta_3^{*}\tau_2\right)-F_{12}\theta_3^{*3}+F_{14}\theta_3^{*},\\
N_{63}(\theta_3^{*})=&\left(G_{12}\theta_3^{*2}-G_{14}\right)\cos\left(\theta_3^{*}\left(\tau_1+\tau_2\right)\right)+\theta_3^{*}\left(G_{11}\theta_3^{*2}-G_{13}\right)\sin\left(\theta_3^{*}\left(\tau_1+\tau_2\right)\right)+\left(-B_{11}\theta_3^{*4}+B_{13}\theta_3^{*2}-B_{15}\right)\cos\left(\theta_3^{*}\tau_1\right)\\
&+\left(-E_{11}\theta_3^{*4}+E_{13}\theta_3^{*2}-E_{15}\right)\cos\left(\theta_3^{*}\tau_2\right)+\theta_3^{*}\left(B_{12}\theta_3^{*2}-B_{14}\right)\sin\left(\theta_3^{*}\tau_1\right)+\theta_3^{*}\left(E_{12}\theta_3^{*2}-E_{14}\right)\sin\left(\theta_3^{*}\tau_2\right)\\
&-A_{11}\theta_3^{*4}+A_{13}\theta_3^{*2}-A_{15},
\end{aligned}
$$

$$N_{64}(\theta_3^*) = \theta_3^*\left(G_{11}\theta_3^{*2} - G_{13}\right)\cos\left(\theta_3^*(\tau_1+\tau_2)\right) + \left(-G_{12}\theta_3^{*2} + G_{14}\right)\sin\left(\theta_3^*(\tau_1+\tau_2)\right) + \sin\left(\theta_3^*\tau_1\right)\left(B_{11}\theta_3^{*4} - B_{13}\theta_3^{*2} + B_{15}\right)$$
$$+ \sin\left(\theta_3^*\tau_2\right)\left(E_{11}\theta_3^{*4} - E_{13}\theta_3^{*2} + E_{15}\right) + \theta_3^*\left(\left(B_{12}\theta_3^{*2} - B_{14}\right)\cos\left(\theta_3^*\tau_1\right) + \left(E_{12}\theta_3^{*2} - E_{14}\right)\cos\left(\theta_3^*\tau_2\right)\right.$$
$$\left. - \theta_3^{*4} + A_{12}\theta_3^{*2} - A_{14}\right).$$

Then, we obtain $N_{63}^2(\theta_3^*) + N_{64}^2(\theta_3^*) - N_{61}^2(\theta_3^*) - N_{62}^2(\theta_3^*) = 0$. Similar to case e, we suppose that $\theta_{31}^*, \theta_{32}^*, \ldots \theta_{3n}^*$ are the finite positive roots of the above equation. Then for θ_{3i}^*, we have $\tau_{3i}^* = \frac{1}{\theta_{3i}^*}\arccos\left[\frac{N_{61}(\theta_3^*)N_{63}(\theta_3^*)+N_{62}(\theta_3^*)N_{64}(\theta_3^*)}{N_{61}^2(\theta_3^*)+N_{62}^2(\theta_3^*)} + 2r\pi\right]$. $i = 1, \ldots, n; \quad r = 0, 1, 2 \ldots$. Proceeding in the same manner as the above case, we suppose that $\tau_3^* = \min\left\{\tau_{3i}^*\right\}$, $i = 1, 2, \ldots, n$. Hence, for $\tau_3 = \tau_3^*$, from Eq. (8), we have $Re\left[\frac{d\lambda}{d\tau_3}\right]^{-1}_{\tau_3=\tau_3^*} = \frac{Y_{61}Y_{63}+Y_{62}Y_{64}}{Y_{61}^2+Y_{62}^2}$ where

$$Y_{61} = \theta_3^*\left(\left(-L_{11}\theta_3^{*2} + L_{13}\right)\sin\left(\theta_3^*(\tau_1+\tau_2+\tau_3^*)\right) - \cos\left(\theta_3^*(\tau_1+\tau_2+\tau_3^*)\right)L_{12}\theta_3^* + \theta_3^*\left(\theta_3^{*2}H_{11} - H_{13}\right)\cos\left(\theta_3(\tau_1+\tau_3^*)\right)\right.$$
$$+ \theta_3^*\left(K_{11}\theta_3^{*2} - K_{13}\right)\cos\left(\theta_3^*(\tau_2+\tau_3^*)\right) + \left(-H_{12}\theta_3^{*2} + H_{14}\right)\sin\left(\theta_3^*(\tau_1+\tau_3^*)\right) + \left(-K_{12}\theta_3^{*2} + K_{14}\right)\sin\left(\theta_3^*(\tau_2+\tau_3^*)\right)$$
$$\left. + \sin\left(\theta_3^*\tau_3^*\right)\left(F_{11}\theta_3^{*4} - F_{13}\theta_3^{*2} + F_{15}\right) + \theta_3^*\cos\left(\theta_3^*\tau_3^*\right)\left(\theta_3^{*2}F_{12} - F_{14}\right)\right),$$
$$Y_{62} = \left(\left(-L_{11}\theta_3^{*2} + L_{13}\right)\cos\left(\theta_3^*(\tau_1+\tau_2+\tau_3^*)\right) + \sin\left(\theta_3^*(\tau_1+\tau_2+\tau_3^*)\right)L_{12}\theta_3^* + \left(-H_{12}\theta_3^{*2} + H_{14}\right)\cos\left(\theta_3^*(\tau_1+\tau_3^*)\right)\right.$$
$$+ \left(-K_{12}\theta_3^{*2} + K_{14}\right)\cos\left(\theta_3^*(\tau_2+\tau_3^*)\right) + \left(-H_{11}\theta_3^{*3} + H_{13}\theta_3^*\right)\sin\left(\theta_3^*(\tau_1+\tau_3^*)\right) + \left(-K_{11}\theta_3^{*3} + K_{13}\theta_3^*\right)\sin\left(\theta_3^*(\tau_2+\tau_3^*)\right)$$
$$\left. + \cos\left(\theta_3^*\tau_3^*\right)\left(F_{11}\theta_3^{*4} - F_{13}\theta_3^{*2} + F_{15}\right) - \theta_3^*\sin\left(\theta_3^*\tau_3^*\right)\left(\theta_3^{*2}F_{12} - F_{14}\right)\right)\theta_3^*,$$
$$Y_{63} = \left(L_{11}\left(\tau_1+\tau_2+\tau_3^*\right)\theta_3^{*2} - L_{13}\tau_1 - L_{13}\tau_2 - L_{13}\tau_3^* + L_{12}\right)\cos\left(\theta_3^*(\tau_1+\tau_2+\tau_3^*)\right)$$
$$+ 2\theta_3^*\left(-1/2\,L_{12}\tau_1 - 1/2\,L_{12}\tau_2 - 1/2\,L_{12}\tau_3^* + L_{11}\right)\sin\left(\theta_3^*(\tau_1+\tau_2+\tau_3^*)\right)$$
$$+ \left(\left(G_{12}\tau_1 + G_{12}\tau_2 - 3\,G_{11}\right)\theta_3^{*2} - G_{14}\tau_1 - G_{14}\tau_2 + G_{13}\right)\cos\left(\theta_3^*(\tau_1+\tau_2)\right)$$
$$+ \left(\left(H_{12}\tau_1 + H_{12}\tau_3^* - 3\,H_{11}\right)\theta_3^{*2} - H_{14}\tau_1 - H_{14}\tau_3^* + H_{13}\right)\cos\left(\theta_3^*(\tau_1+\tau_3^*)\right)$$
$$+ \left(\left(K_{12}\tau_2 + K_{12}\tau_3^* - 3\,K_{11}\right)\theta_3^{*2} - K_{14}\tau_2 - K_{14}\tau_3^* + K_{13}\right)\cos\left(\theta_3^*(\tau_2+\tau_3^*)\right)$$
$$+ \theta_3^*\left(G_{11}\left(\tau_1+\tau_2\right)\theta_3^{*2} - G_{13}\tau_1 - G_{13}\tau_2 + 2\,G_{12}\right)\sin\left(\theta_3^*(\tau_1+\tau_2)\right)$$
$$+ \theta_3^*\left(H_{11}\left(\tau_1+\tau_3^*\right)\theta_3^{*2} - H_{13}\tau_1 - H_{13}\tau_3^* + 2\,H_{12}\right)\sin\left(\theta_3^*(\tau_1+\tau_3^*)\right)$$
$$+ \theta_3^*\left(K_{11}\left(\tau_2+\tau_3^*\right)\theta_3^{*2} - K_{13}\tau_2 - K_{13}\tau_3^* + 2\,K_{12}\right)\sin\left(\theta_3^*(\tau_2+\tau_3^*)\right)$$
$$+ \left(-B_{11}\tau_1\theta_3^{*4} + \left(B_{13}\tau_1 - 3\,B_{12}\right)\theta_3^{*2} - B_{15}\tau_1 + B_{14}\right)\cos\left(\theta_3^*\tau_1\right)$$
$$+ \left(-E_{11}\tau_2\theta_3^{*4} + \left(E_{13}\tau_2 - 3\,E_{12}\right)\theta_3^{*2} - E_{15}\tau_2 + E_{14}\right)\cos\left(\theta_3^*\tau_2\right)$$
$$+ \left(-F_{11}\tau_3^*\theta_3^{*4} + \left(F_{13}\tau_3^* - 3\,F_{12}\right)\theta_3^{*2} - F_{15}\tau_3^* + F_{14}\right)\cos\left(\theta_3^*\tau_3^*\right)$$
$$- 4\left(\left(-1/4\,\tau_1 B_{12} + B_{11}\right)\theta_3^{*2} + 1/4\,\tau_1 B_{14} - 1/2\,B_{13}\right)\theta_3^*\sin\left(\theta_3^*\tau_1\right)$$
$$+ 2\left(\left(1/2\,\tau_2 E_{12} - 2\,E_{11}\right)\theta_3^{*2} - 1/2\,E_{14}\tau_2 + E_{13}\right)\theta_3^*\sin\left(\theta_3^*\tau_2\right)$$
$$- 4\theta_3^*\left(\left(-1/4\,F_{12}\tau_3^* + F_{11}\right)\theta_3^{*2} + 1/4\,F_{14}\tau_3 - 1/2\,F_{13}\right)\sin\left(\theta_3^*\tau_3^*\right) + 5\,\theta_3^{*4} - 3\,A_{12}\theta_3^{*2} + A_{14},$$
$$Y_{64} = \left(-L_{11}\left(\tau_1+\tau_2+\tau_3^*\right)\theta_3^{*2} + L_{13}\tau_1 + L_{13}\tau_2 + L_{13}\tau_3^* - L_{12}\right)\sin\left(\theta_3^*(\tau_1+\tau_2+\tau_3^*)\right)$$
$$+ 2\theta_3^*\left(-1/2\,L_{12}\tau_1 - 1/2\,L_{12}\tau_2 - 1/2\,L_{12}\tau_3^* + L_{11}\right)\cos\left(\theta_3^*(\tau_1+\tau_2+\tau_3^*)\right)$$
$$+ \left(\left(-G_{12}\tau_1 - G_{12}\tau_2 + 3\,G_{11}\right)\theta_3^{*2} + G_{14}\tau_1 + G_{14}\tau_2 - G_{13}\right)\sin\left(\theta_3^*(\tau_1+\tau_2)\right)$$
$$+ \left(\left(-H_{12}\tau_1 - H_{12}\tau_3^* + 3\,H_{11}\right)\theta_3^{*2} + H_{14}\tau_1 + H_{14}\tau_3^* - H_{13}\right)\sin\left(\theta_3^*(\tau_1+\tau_3^*)\right)$$
$$+ \left(\left(-K_{12}\tau_2 - K_{12}\tau_3^* + 3\,K_{11}\right)\theta_3^{*2} + K_{14}\tau_2 + K_{14}\tau_3^* - K_{13}\right)\sin\left(\theta_3^*(\tau_2+\tau_3^*)\right)$$
$$+ \theta_3^*\left(G_{11}\left(\tau_1+\tau_2\right)\theta_3^{*2} - G_{13}\tau_1 - G_{13}\tau_2 + 2\,G_{12}\right)\cos\left(\theta_3^*(\tau_1+\tau_2)\right)$$

$$
\begin{aligned}
&+\theta_3^*\left(H_{11}\left(\tau_1+\tau_3^*\right)\theta_3^{*2}-H_{13}\tau_1-H_{13}\tau_3^*+2\,H_{12}\right)\cos\left(\theta_3^*\left(\tau_1+\tau_3^*\right)\right)\\
&+\theta_3^*\left(K_{11}\left(\tau_2+\tau_3^*\right)\theta_3^{*2}-K_{13}\tau_2-K_{13}\tau_3^*+2\,K_{12}\right)\cos\left(\theta_3^*\left(\tau_2+\tau_3^*\right)\right)\\
&+\left(B_{11}\tau_1\theta_3^{*4}+\left(-B_{13}\tau_1+3\,B_{12}\right)\theta_3^{*2}+B_{15}\tau_1-B_{14}\right)\sin\left(\theta_3^*\tau_1\right)\\
&+\left(E_{11}\tau_2\theta_3^{*4}+\left(-E_{13}\tau_2+3\,E_{12}\right)\theta_3^{*2}+E_{15}\tau_2-E_{14}\right)\sin\left(\theta_3^*\tau_2\right)\\
&+\left(F_{11}\tau_3^*\theta_3^{*4}+\left(-F_{13}\tau_3^*+3\,F_{12}\right)\theta_3^{*2}+F_{15}\tau_3^*-F_{14}\right)\sin\left(\theta_3^*\tau_3^*\right)\\
&-4\,\theta_3^*\Big(\left(\left(-1/4\,\tau_1B_{12}+B_{11}\right)\theta_3^{*2}+1/4\,\tau_1B_{14}-1/2\,B_{13}\right)\cos\left(\theta_3^*\tau_1\right)\\
&+\left(\left(E_{11}-1/4\,\tau_2E_{12}\right)\theta_3^{*2}+1/4\,E_{14}\tau_2-1/2\,E_{13}\right)\cos\left(\theta_3^*\tau_2\right)\\
&+\left(\left(-1/4\,F_{12}\tau_3^*+F_{11}\right)\theta_3^{*2}+1/4\,F_{14}\tau_3^*-1/2\,F_{13}\right)\cos\left(\theta_3^*\tau_3^*\right)-1/2\,A_{13}+A_{11}\theta_3^{*2}\Big).
\end{aligned}
$$

Clearly, when $Y_{61}Y_{63}+Y_{62}Y_{64}\neq 0$ then, $\mathrm{Re}[d\lambda/d\tau_3]^{-1}_{\tau_3=\tau_3^*}\neq 0$. Thus, we have the Theorem 3(f).

Declarations

Use of AI tools

The authors declare that they have not used Artificial Intelligence (AI) tools in the creation of this article.

Data availability statement

The data that support the findings of this study are openly available from the World Health Organization website. https://covid19.who.int/WHO-COVID-19-global-data.csv

Ethical approval (optional)

The authors state that this research complies with ethical standards. This research does not involve either human participants or animals.

Consent for publication

Not applicable

Conflicts of interest

The authors declare that they have no conflict of interest.

Funding

This research was supported by the National Board for Higher Mathematics, Department of Atomic Energy, Mumbai, India, under the grant no. 02011/8/2020/NBHM/R&D-II/8071.

Author's contributions

B.K.: Conceptualization, Methodology, Investigation, Visualization, Writing – original draft. P.T.: Conceptualization, Methodology, Investigation, Visualization, Writing – original draft, Supervision. The authors have read and agreed to the published version of the manuscript.

Acknowledgements

Not applicable

References

[1] Goel, K., Kumar, A. and Nilam. A deterministic time-delayed SVIRS epidemic model with incidences and saturated treatment. *Journal of Engineering Mathematics*, 121, 19-38, (2020). [CrossRef]

[2] Guo, S., Xue, Y., Yuan, R. and Liu, M. An improved method of global dynamics: Analyzing the COVID-19 model with time delays and exposed infection. *Chaos: An Interdisciplinary Journal of Nonlinear Science*, 33(5), 053116, (2023). [CrossRef]

[3] Mvogo, A., Tiomela, S.A., Macías-Díaz, J.E. and Bertrand, B. Dynamics of a cross-superdiffusive SIRS model with delay effects in transmission and treatment. *Nonlinear Dynamics*, 111, 13619-13639, (2023). [CrossRef]

[4] Singh, A. and Arquam, M. Epidemiological modeling for COVID-19 spread in India with the effect of testing. *Physica A: Statistical Mechanics and its Applications*, 592, 126774, (2022). [CrossRef]

[5] Tamilalagan, P., Krithika, B., Manivannan, P. and Karthiga, S. Is reinfection negligible effect in COVID-19? A mathematical study on the effects of reinfection in COVID-19. *Mathematical Methods in the Applied Sciences*, 46(18), 19115-19134, (2023). [CrossRef]

[6] Garba, S.M., Lubuma, J.M.S. and Tsanou, B. Modeling the transmission dynamics of the COVID-19 Pandemic in South Africa. *Mathematical Biosciences*, 328, 108441, (2020). [CrossRef]

[7] Taboe, H.B., Salako, K.V., Tison, J.M., Ngonghala, C.N. and Kakaï, R.G. Predicting COVID-19 spread in the face of control measures in West Africa. *Mathematical Biosciences*, 328, 108431, (2020). [CrossRef]

[8] Ngonghala, C.N., Taboe, H.B., Safdar, S. and Gumel, A.B. Unraveling the dynamics of the Omicron and Delta variants of the 2019 coronavirus in the presence of vaccination, mask usage, and antiviral treatment. *Applied Mathematical Modelling*, 114, 447-465, (2023). [CrossRef]

[9] Wang, K., Fan, H. and Zhu, Y. Dynamics and application of a generalized SIQR epidemic model with vaccination and treatment. *Applied Mathematical Modelling*, 120, 382-399, (2023). [CrossRef]

[10] Ojo, M.M., Peter, O.J., Goufo, E.F.D. and Nisar, K.S. A mathematical model for the co-dynamics of COVID-19 and tuberculosis. *Mathematics and Computers in Simulation*, 207, 499-520, (2023). [CrossRef]

[11] Chen, Z., Feng, L., Lay Jr, H.A., Furati, K. and Khaliq, A. SEIR model with unreported infected population and dynamic parameters for the spread of COVID-19. *Mathematics and Computers in Simulation*, 198, 31-46, (2022).

[12] Saha, S., Samanta, G. and Nieto, J.J. Impact of optimal vaccination and social distancing on COVID-19 pandemic. *Mathematics and Computers in Simulation*, 200, 285-314, (2022). [CrossRef]

[13] Peter, O.J., Abidemi, A., Fatmawati, F., Ojo, M.M. and Oguntolu, F.A. Optimizing tuberculosis control: a comprehensive simulation of integrated interventions using a mathematical model. *Mathematical Modelling and Numerical Simulation with Applications*, 4(3), 238-255, (2024). [CrossRef]

[14] Ouaziz, S.I. and El Khomssi, M. Mathematical approaches to controlling COVID-19: optimal control and financial benefits. *Mathematical Modelling and Numerical Simulation with Applications*, 4(1), 1-36, (2024). [CrossRef]

[15] Mustapha, U.T., Ado, A., Yusuf, A., Qureshi, S. and Musa, S.S. Mathematical dynamics for HIV infections with public awareness and viral load detectability. *Mathematical Modelling and Numerical Simulation with Applications*, 3(3), 256-280, (2023). [CrossRef]

[16] Pérez, A.G.C. and Oluyori, D.A. A model for COVID-19 and bacterial pneumonia coinfection with community- and hospital-acquired infections. *Mathematical Modelling and Numerical Simulation with Applications*, 2(4), 197-210, (2022). [CrossRef]

[17] Turan, M., Sevinik Adıgüzel, R. and Koç, F. Stability analysis of an epidemic model with vaccination and time delay. *Mathematical Methods in the Applied Sciences*, 46(14), 14828-14840, (2023). [CrossRef]

[18] Zhang, Z., Zhang, W., Nisar, K.S., Gul, N., Zeb, A. and Vijayakumar, V. Dynamical aspects of a tuberculosis transmission model incorporating vaccination and time delay. *Alexandria Engineering Journal*, 66, 287-300, (2023). [CrossRef]

[19] Sepulveda, G., Arenas, A.J. and González-Parra, G. Mathematical modeling of COVID-19 dynamics under two vaccination doses and delay effects. *Mathematics*, 11(2), 369, (2023). [CrossRef]

[20] Marot, S., Malet, I., Leducq, V., Zafilaza, K., Sterlin, D., Planas, D. et al. Rapid decline of neutralizing antibodies against SARS-CoV-2 among infected healthcare workers. *Nature Communications*, 12, 844, (2021). [CrossRef]

[21] Prather, A.A., Dutcher, E.G., Robinson, J., Lin, J., Blackburn, E., Hecht, F.M. et al. Predictors of long-term neutralizing antibody titers following COVID-19 vaccination by three vaccine types: the BOOST study. Scientific reports, 13, 6505, (2023). [CrossRef]

[22] Puthiyedath, R., Kataria, S., Payyappallimana, U., Mangalath, P., Nampoothiri, V., Sharma, P. et al. Ayurvedic clinical profile of COVID-19–a preliminary report. *Journal of Ayurveda and Integrative Medicine*, 13(1), 100326, (2022). [CrossRef]

[23] Tamilalagan, P., Karthiga, S. and Manivannan, P. Dynamics of fractional order HIV infection model with antibody and cytotoxic T-lymphocyte immune responses. *Journal of Computational and Applied Mathematics*, 382, 113064, (2021). [CrossRef]

[24] Cerón Gómez, M. and Yang, H.M. A simple mathematical model to describe antibody-dependent enhancement in heterologous secondary infection in dengue. *Mathematical Medicine and Biology: A Journal of the IMA*, 36(4), 411-438, (2019). [CrossRef]

[25] Katriel, G. Epidemics with partial immunity to reinfection. *Mathematical Biosciences*, 228(2), 153-159, (2010). [CrossRef]

[26] Hethcote, H.W. The mathematics of infectious diseases. *SIAM Review*, 42(4), 599-653, (2000). [CrossRef]

[27] Pathak, S., Maiti, A. and Samanta, G.P.P. Rich dynamics of an SIR epidemic model. *Nonlinear Analysis: Modelling and Control*, 15(1), 71-81, (2010). [CrossRef]

[28] Hassard, B.D., Kazarinoff, N.D. and Wan, Y.H. *Theory and Applications of Hopf Bifurcation* (Vol. 41). Cambridge University Press: New York, (1981).

[29] Zhang, Z., Kundu, S., Tripathi, J.P. and Bugalia, S. Stability and Hopf bifurcation analysis of an SVEIR epidemic model with vaccination and multiple time delays. *Chaos, Solitons & Fractals*, 131, 109483, (2020). [CrossRef]

[30] Danchin, A. and Turinici, G. Immunity after COVID-19: Protection or sensitization? *Mathematical Biosciences*, 331, 108499, (2021). [CrossRef]

[31] Papageorgiou, V.E. and Tsaklidis, G. A stochastic SIRD model with imperfect immunity for the evaluation of epidemics. *Applied Mathematical Modelling*, 124, 768-790, (2023). [CrossRef]

[32] Sharma, S. and Samanta, G.P. Stability analysis and optimal control of an epidemic model with vaccination. *International Journal of Biomathematics*, 8(03), 1550030, (2015). [CrossRef]

[33] Sasidharakurup, H., Kumar, G., Nair, B. and Diwakar, S. Mathematical modeling of severe acute respiratory syndrome coronavirus 2 infection network with cytokine storm, oxidative stress, thrombosis, insulin resistance, and nitric oxide pathways. *OMICS: A Journal of Integrative Biology*, 25(12), 770-781, (2021). [CrossRef]

[34] Narassima, M.S., John, D., Anbuudayasankar, S.P., Jammy, G.R., Pant, R. and Choudhury, L. SHIVIR-An Agent-Based Model to assess the transmission of COVID-19 in India. *MedRxiv*, 1-26, (2022). [CrossRef]

[35] Li, Q., Tang, B., Bragazzi, N.L., Xiao, Y. and Wu, J. Modeling the impact of mass influenza vaccination and public health interventions on COVID-19 epidemics with limited detection capability. *Mathematical Biosciences*, 325, 108378, (2020). [CrossRef]

[36] Tchoumi, S.Y., Diagne, M.L., Rwezaura, H. and Tchuenche, J.M. Malaria and COVID-19 co-dynamics: A mathematical model and optimal control. *Applied Mathematical Modelling*, 99, 294-327, (2021). [CrossRef]

[37] Baba, I.A., Humphries, U.W. and Rihan, F.A. Role of vaccines in controlling the spread of COVID-19: A fractional-order model. *Vaccines*, 11(1), 145, (2023). [CrossRef]

[38] Saiprasad, V.R., Gopal, R., Chandrasekar, V.K. and Lakshmanan, M. Analysis of COVID-19 in India using a vaccine epidemic model incorporating vaccine effectiveness and herd immunity. *The European Physical Journal Plus*, 137, 1003, (2022). [CrossRef]

[39] Balasubramaniam, P., Prakash, M. and Tamilalagan, P. Stability and Hopf bifurcation analysis of immune response delayed HIV type 1 infection model with two target cells. *Mathematical Methods in the Applied Sciences*, 38(17), 3653-3669, (2015). [CrossRef]

[40] Balasubramaniam, P., Tamilalagan, P. and Prakash, M. Bifurcation analysis of HIV infection model with antibody and cytotoxic T-lymphocyte immune responses and Beddington–DeAngelis functional response. *Mathematical Methods in the Applied Sciences*, 38(7), 1330-1341, (2015). [CrossRef]

[41] Khajanchi, S. Bifurcation analysis of a delayed mathematical model for tumor growth. *Chaos, Solitons & Fractals*, 77, 264-276, (2015). [CrossRef]

[42] Misra, A. K. and Singh, V. A delay mathematical model for the spread and control of water borne diseases. *Journal of Theoretical Biology*, 301, 49-56, (2012). [CrossRef]

[43] Zhang, T., Li, Z., Ma, L. and Song, X. Threshold dynamics in a clonorchiasis model with time delays. *Applied Mathematical Modelling*, 102, 351-370, (2022). [CrossRef]

[44] Cumsille, P., Rojas-Díaz, Ó., de Espanés, P.M. and Verdugo-Hernández, P. Forecasting COVID-19 Chile'second outbreak by a generalized SIR model with constant time delays and a fitted positivity rate. *Mathematics and*

Computers in Simulation, 193, 1-18, (2022). [CrossRef]

[45] Matrajt, L., Britton, T., Halloran, M.E. and Longini Jr, I.M. One versus two doses: What is the best use of vaccine in an influenza pandemic? *Epidemics*, 13, 17-27, (2015). [CrossRef]

[46] Liu, X., Takeuchi, Y. and Iwami, S. SVIR epidemic models with vaccination strategies. *Journal of Theoretical Biology*, 253(1), 1-11, (2008). [CrossRef]

[47] Kim, Y., Bae, S., Chang, H.H. and Kim, S.W. Characteristics of long COVID and the impact of COVID-19 vaccination on long COVID 2 years following COVID-19 infection: prospective cohort study. *Scientific Reports*, 14, 854, (2024). [CrossRef]

[48] Cai, L.M., Li, Z. and Song, X. Global analysis of an epidemic model with vaccination. *Journal of Applied Mathematics and Computing*, 57, 605-628, (2018). [CrossRef]

[49] Liu, Z., Magal, P., Seydi, O. and Webb, G. A COVID-19 epidemic model with latency period. *Infectious Disease Modelling*, 5, 323-337, (2020). [CrossRef]

[50] FAQs on COVID-19 Vaccines and Vaccination Program-India, (2020). https://www.mohfw.gov.in/pdf/FAQsCOVID19vaccinesvaccinationprogramWebsiteupload27Sep.pdf

[51] Antia, A., Ahmed, H., Handel, A., Carlson, N.E., Amanna, I.J., Antia, R. and Slifka, M. Heterogeneity and longevity of antibody memory to viruses and vaccines. *PLoS Biology*, 16(8), e2006601, (2018). [CrossRef]

[52] Van den Driessche, P. and Watmough, J. Reproduction numbers and sub-threshold endemic equilibria for compartmental models of disease transmission. *Mathematical Biosciences*, 180(1-2), 29-48, (2002). [CrossRef]

[53] Diekmann, O., Heesterbeek, J.A.P. and Metz, J.A.J. On the definition and the computation of the basic reproduction ratio R_0 in models for infectious diseases in heterogeneous populations. *Journal of Mathematical Biology*, 28, 365-382, (1990). [CrossRef]

[54] Li, C.K. and Schneider, H. Applications of Perron-Frobenius theory to population dynamics. *ArXiv Prints, ArXiv:math/0109008*, (2001). [CrossRef]

[55] Brouwer, A.F. Why the Spectral Radius? An intuition-building introduction to the basic reproduction number. *Bulletin of Mathematical Biology*, 84, 96, (2022). [CrossRef]

[56] Worldometer, Covid-19 Coronavirus Pandemic, (2024). https://www.worldometers.info/coronavirus/?utm_cam-paign=homeAdvegas1?

[57] Countrymeters, India Population, (2025). https://countrymeters.info/en/India.

[58] World Bank Group, Life expectancy at birth, total (years)-India, (2023). https://data.worldbank.org/indicator/SP.DYN.LE00.IN?locations=IN

[59] Wu, J., Dhingra, R., Gambhir, M. and Remais, J.V. Sensitivity analysis of infectious disease models: methods, advances and their application. *Journal of The Royal Society Interface*, 10(86), 20121018, (2013). [CrossRef]

[60] Powell, D.R., Fair, J., LeClaire, R.J., Moore, L.M. and Thompson, D. Sensitivity analysis of an infectious disease model. In Proceedings, *International System Dynamics Conference*, pp. 1-20, Boston, USA, (2005, July).

Mathematical Modelling and Numerical Simulation with Applications (MMNSA)
(https://dergipark.org.tr/en/pub/mmnsa)

How to cite this article: Krithika, B. & Tamilalagan, P. (2025). Temporal dynamics of immunity: modeling susceptibility delay in antibody-shielded populations. *Mathematical Modelling and Numerical Simulation with Applications*, 5(2), 280-306. https://doi.org/10.53391/mmnsa.1567457